AMERICAN SOCIETY FOR MICROBIOLOGY | Journal of Virology®

VIRUS-CELL INTERACTIONS

HACE1, an E3 Ubiquitin Protein Ligase, Mitigates Kaposi's Sarcoma-Associated Herpesvirus Infection-Induced Oxidative Stress by Promoting Nrf2 Activity

Binod Kumar,[a] Arunava Roy,[a,c] Kumari Asha,[a] Neelam Sharma-Walia,[a] Mairaj Ahmed Ansari,[a]* Bala Chandran[a,c]

[a]Department of Microbiology and Immunology, Chicago Medical School, Rosalind Franklin University of Medicine and Science, North Chicago, Illinois, USA
[b]Immunology Division, National JALMA Institute for Leprosy and Other Mycobacterial Diseases (ICMR), Tajganj, Agra, India
[c]Department of Molecular Medicine, Morsani College of Medicine, University of South Florida, Tampa, Florida, USA

ABSTRACT Kaposi's sarcoma-associated herpesvirus (KSHV)-induced activation of nuclear factor erythroid 2-related factor 2 (Nrf2) is essential for both the expression of viral genes (latency) and modulation of the host antioxidant machinery. Reactive oxygen species (ROS) are also regulated by the ubiquitously expressed HACE1 protein (HECT domain and ankyrin repeat containing E3 ubiquitin protein ligase 1), which targets the Rac1 protein for proteasomal degradation, and this blocks the generation of ROS by Rac1-dependent NADPH oxidases. In this study, we examined the role of HACE1 in KSHV infection. Elevated levels of HACE1 expression were observed in *de novo* KSHV-infected endothelial cells, KSHV latently infected TIVE-LTC and PEL cells, and Kaposi's sarcoma skin lesion cells. The increased HACE1 expression in the infected cells was mediated by KSHV latent protein kaposin A. HACE1 knockdown resulted in high Rac1 and Nox 1 (NADPH oxidase 1) activity, increased ROS (oxidative stress), increased cell death, and decreased KSHV gene expression. Loss of HACE1 impaired KSHV infection-induced phosphoinositide 3-kinase (PI3-K), protein kinase C-ζ (PKC-ζ), extracellular signal-regulated kinase 1/2 (ERK1/2), NF-κB, and Nrf2 activation and nuclear translocation of Nrf2, and it reduced the expression of Nrf2 target genes responsible for balancing the oxidative stress. In the absence of HACE1, glutamine uptake increased in the cells to cope with the KSHV-induced oxidative stress. These findings reveal for the first time that HACE1 plays roles during viral infection-induced oxidative stress and demonstrate that HACE1 facilitates resistance to KSHV infection-induced oxidative stress by promoting Nrf2 activity. Our studies suggest that HACE1 could be a potential target to induce cell death in KSHV-infected cells and to manage KSHV infections.

IMPORTANCE ROS play important roles in several cellular processes, and increased ROS cause several adverse effects. KSHV infection of endothelial cells induces ROS, which facilitate virus entry by amplifying the infection-induced host cell signaling cascade, which, in turn, induces the nuclear translocation of phospho-Nrf2 protein to regulate the expression of antioxidative genes and viral genes. The present study demonstrates that KSHV infection induces the E3 ligase HACE1 protein to regulate KSHV-induced oxidative stress by promoting the activation of Nrf2 and nuclear translocation. Absence of HACE1 results in increased ROS and cellular death and reduced nuclear Nrf2, antioxidant, and viral gene expression. Together, these studies suggest that HACE1 can be a potential target to induce cell death in KSHV-infected cells.

KEYWORDS HACE1 and KSHV, KSHV and ROS, Nrf2 and KSHV

Citation Kumar B, Roy A, Asha K, Sharma-Walia N, Ansari MA, Chandran B. 2019. HACE1, an E3 ubiquitin protein ligase, mitigates Kaposi's sarcoma-associated herpesvirus infection-induced oxidative stress by promoting Nrf2 activity. J Virol 93:e01812-18. https://doi.org/10.1128/JVI.01812-18.

Editor Jae U. Jung, University of Southern California

Address correspondence to Binod Kumar, binod.kumar@rosalindfranklin.edu, or Bala Chandran, chandran@health.usf.edu.

* Present address: Mairaj Ahmed Ansari, Department of Biotechnology, Jamia Hamdard, New Delhi, India.

Received 10 October 2018
Accepted 12 February 2019
Accepted manuscript posted online 20 February 2019
Published 17 April 2019

Kaposi's sarcoma-associated herpesvirus (KSHV) is etiologically associated with human malignancies such as the angioproliferative Kaposi's sarcoma (KS), primary effusion B-cell lymphoma (PEL) or body cavity B-cell lymphoma (BCBL), and plasmablastic multicentric Castleman's disease (MCD) (1, 2). Multiple copies of latent KSHV genomes are detected in the KS lesion endothelial cells and in the B cells of PEL and MCD lesions (3–5). Human BCBL-1 and BC-3 B-cell lines from PEL carry latent KSHV genomes and express several latency-associated proteins, such as ORF73 (latency-associated nuclear antigen 1 [LANA-1]), as well as 12 microRNAs (3–5). KS lesions are characterized by the hyperplastic spindle-shaped cells of endothelial origin along with a heterogeneous environment of neovascular structures, inflammatory cells, cytokines, growth factors, and angiogenic factors (3–5). KSHV *de novo* infection of primary human dermal microvascular endothelial (HMVEC-d) cells, used as one of the *in vitro* models of infection of endothelial cells, results in a concurrent expression of the latent genes and a limited set of lytic genes with antiapoptotic and immune-evasive roles (6). KSHV infection of HMVEC-d cells also induces several inflammatory cytokines, growth factors, and angiogenic factors, such as interleukin 1β (IL-1β), IL-18, IL-2, IL-6, COX-2, prostaglandin E_2 (PGE_2), vascular endothelial growth factor A/C (VEGFA/C), angiogenin, and gamma interferon (IFN-γ), in the supernatants, which are similar to the microenvironments observed in the KS and PEL lesions and are the driving force of the pathogenesis (7–9).

Reactive oxygen species (ROS) are well-known stress-associated agents which mediate important roles in cell signaling and homeostasis. ROS also play critical roles in KSHV pathogenesis and oxidative stress and have been shown to reactivate KSHV from latency in endothelial and PEL cells (10, 11). In the KSHV-infected endothelial cell latency model, activation of the Rac1 (Ras-related C3 botulinum toxin substrate 1)-NADPH (NADP) oxidase-ROS pathway was observed and led to the phosphorylation of junctional VE-cadherin and β-catenin proteins, disassembly of cell junctions, and increased vascular permeability of the infected endothelial cells (12). In a PEL mouse model, inhibition of ROS by the antioxidant *N*-acetylcysteine (NAC) prevented the tumorigenesis of KSHV and extended the life span of mice (11). NAC treatment also inhibited the tumor size in an endothelial KS-mouse model (13).

KSHV enters HMVEC-d cells via macropinocytosis, which is initiated by the binding of KSHV envelope glycoproteins with cell surface heparan sulfate, integrins ($\alpha3\beta1$, $\alpha V\beta3$, and $\alpha V\beta5$), and ephrin-A2 tyrosine kinase receptor (EphA2R), which induces the host cell preexisting focal adhesion kinase (FAK), Src, c-Cbl, phosphoinositide 3-kinase (PI3-K), Rho A and Rac-1 GTPases, and ROS (14, 15). Consequently, the downstream target molecules, such as protein kinase C-ζ (PKC-ζ), extracellular signal-regulated kinase 1/2 (ERK1/2), NF-κB, and p38 mitogen-activated protein kinase (p38 MAPK), are activated, which collectively create a microenvironment required for virus entry, delivery of viral double-stranded DNA (dsDNA) into the nucleus, viral gene expression, and the establishment of KSHV latency (16–18). In addition, virus binding and entry also activate the COX-2–PGE_2 pathway, and during latency, this pathway is activated via the KSHV latent protein vFLIP (19). Several studies have shown that the COX-2–PGE_2 pathway is essential for viral latent gene expression and maintenance (7, 17). KSHV binding to HMVEC-d cells also induced the production of ROS; this production was sustained until 24 h postinfection (p.i.), a time at which KSHV has established latent gene expression (14). Pretreatment of HMVEC-d cells with NAC significantly inhibited KSHV entry and gene expression, and H_2O_2 treatment increased KSHV entry and gene expression. NAC inhibited the activation of EphA2R, FAK, Src, and Rac1, while H_2O_2 treatment increased the activation of these molecules, thus demonstrating that KSHV infection induces ROS to amplify the signaling pathways necessary for its efficient entry and viral gene expression (14).

One of the downstream targets of ROS is nuclear factor erythroid 2-related factor 2 (Nrf2), which is a master regulator of the antioxidative stress with its activity tightly regulated by the cellular redox balance (20, 21). Under physiological conditions, Nrf2 is bound to the oxidative stress sensor KEAP1, which promotes ubiquitylation and

proteasomal degradation of Nrf2 and thus keeps the Nrf2 at a low basal activity (22). During oxidative stress, including KSHV *de novo* infection, KEAP1 is oxidized and disassociates from Nrf2, leading to the phosphorylation and nuclear translocation of Nrf2 and the expression of Nrf2 target genes such as those encoding the antioxidant proteins HO1 (heme oxygenase 1), NQO1 (NAD[P]H dehydrogenase 1), and GSS (glutathione [GSH] synthetase). Besides the KEAP1-mediated regulation of Nrf2, p21 and p62 proteins also interfere with KEAP1 binding to NRF2 (23, 24). H_2O_2 as well as the Ras pathway increases the Nrf2 mRNA translation and Nrf2 accumulation (25).

We have previously observed that *de novo* infection of HMVEC-d cells require ROS for Nrf2 activation during the early stages of infection and establishment of latency (26). We also observed an elevated activated Nrf2 levels in KSHV positive KS and PEL lesion cells (26). Our subsequent studies in the long-term-infected telomerase-immortalized endothelial (TIVE-LTC) cells identified the existence of two simultaneous Nrf2 activation pathways necessary for the sustained expression of Nrf2 target genes such as those encoding GCS, NQO1, xCT, VEGF, and IL-6, which are the key mediators of KSHV pathogenesis and oncogenesis (27). Our studies have also demonstrated the colocalization of Nrf2 with the KSHV genome and the LANA-1 protein during latency as well as the interactions of Nrf2 with ORF73 (latent) and ORF50 (lytic) promoters to collectively utilize Nrf2's functions for its survival advantage (28).

Recent studies demonstrated that ROS are also regulated by another key molecule known as HACE1 (HECT domain and ankyrin repeat containing E3 ubiquitin protein ligase 1). HACE1, initially identified in the context of Wilms' tumor (29), has been shown to act as a tumor suppressor in multiple cancers (30). HACE1 is a ubiquitously expressed E3 ubiquitin-protein ligase involved in Golgi membrane fusion and the regulation of small GTPases (31). HACE1 specifically ubiquitylates the activated GTP-bound form of the Rac1GTPase protein, resulting in the proteasomal degradation of Rac1 (32). HACE1 targets the Rac1 protein when it is localized to the NADPH oxidase holoenzyme and thus blocks ROS generation by Rac1-dependent NADPH oxidases (14). Studies have also shown a similarity of tumor enhancement function between Nrf2 and HACE1 in mice subjected to ionizing radiations (30). Another study revealed that HACE1 promotes the stability of Nrf2 and thus plays an important role in the antioxidant response in Huntington disease (33, 34). However, the role of HACE1 in viral infection-induced oxidative stress is not known.

As HACE1 plays a critical role during ROS-mediated oxidative stress, we examined its role in KSHV-induced oxidative stress and Nrf2 activation. We observed a significant increase in the expression of HACE1 upon KSHV infection, and its loss greatly impaired viral gene expression by dampening the KSHV-induced signal pathways and Nrf2 pathway. Our results also demonstrate that HACE1 plays a crucial role in mitigating KSHV-induced oxidative stress by promoting Nrf2 activity.

RESULTS

KSHV-infected cells exhibit higher expression of HACE1. Persistent inflammation and increased oxidative stress by reactive oxygen species have been shown to be some of the key factors in the development of KSHV-associated endothelial KS and PEL B lymphoma (35). KSHV *de novo* infection induces ROS, which, in turn, induce EphA2R, FAK, Src, and Rac1 signal molecules to aid in virus entry, nuclear viral DNA entry, and viral gene expression (14). Our studies have also demonstrated that *de novo* KSHV-infected endothelial cells, KSHV-positive endothelial cells of patients' KS lesions, and B cells of PEL lesions, as well as KSHV latently infected PEL cell lines, express higher levels of Nrf2, the master regulator of the antioxidative stress response (26–28). As HACE1 has been shown to mediate a protective antioxidative role by controlling Rac1 activity to maintain the ROS homeostasis, we determined the role of HACE1 in KSHV biology.

Western blot (WB) analyses of endothelial hTERT-immortalized microvascular endothelial (TIME) cells infected with KSHV (30 DNA copies/cell) for 4 h demonstrated a significant increase in HACE1 protein in infected cells compared to the uninfected cells (Fig. 1A). In an immunofluorescence assay (IFA), we observed a prominent increase in

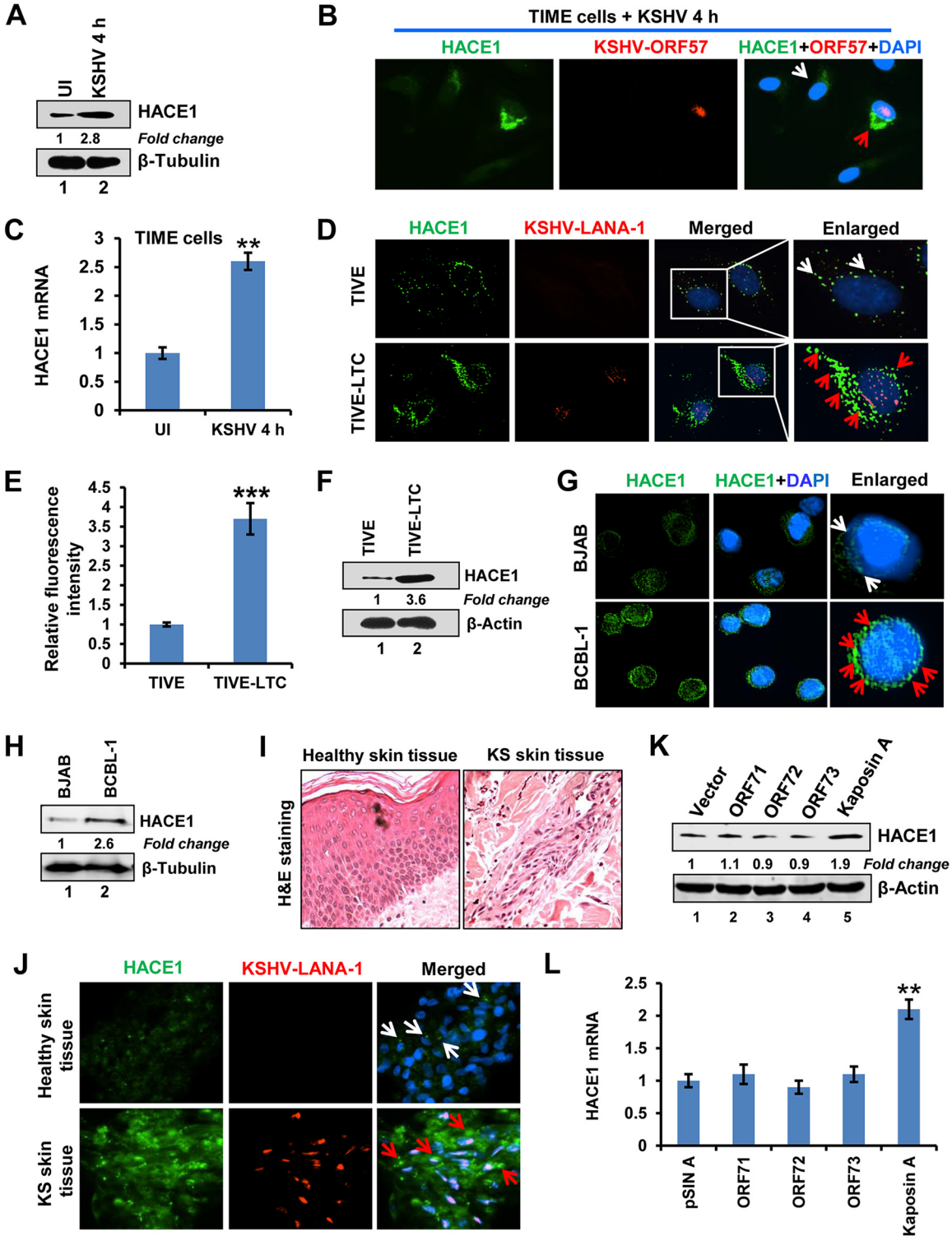

FIG 1 Demonstration of increased HACE1 expression during KSHV infection. (A) TIME cells were either left uninfected or infected with KSHV (30 DNA copies/cell) for 4 h and Western blotted (WB) with anti-HACE1 antibody. β-Tubulin was used as a loading control. Fold inductions were normalized to β-tubulin and calculated relative to the uninfected (UI) condition, arbitrarily set to 1. (B) Immunofluorescence analysis of KSHV (30 DNA copies/cell)-infected TIME cells with anti-HACE1 and anti-KSHV immediate early protein ORF57 antibodies. DAPI was used to visualize the nuclei. The white arrow indicates lower expression of HACE1 in uninfected cells, while the red arrow shows increased HACE1 expression in KSHV-infected TIME cells. (C) Real-time RT-PCR analysis of HACE1 mRNA at 4 h after KSHV infection of TIME cells. Results presented are means ± SD of three independent experiments. **, $P < 0.01$. (D) Immunofluorescence analysis of TIVE and KSHV latency TIVE-LTC cells by incubation with rabbit anti-HACE1 antibody and then with goat anti-rabbit (Alexa Fluor 488 [green]) secondary antibody. KSHV LANA-1 was stained using mouse anti-LANA-1 followed by goat anti-mouse (Alexa Fluor 594 [red]) secondary antibody. DAPI was used to visualize the nuclei. The white arrows indicate lower expression of HACE1 in TIVE cells, while the red arrows

(Continued on next page)

HACE1 protein expression in the KSHV-infected cells as measured by the detection of KSHV immediate early (IE) ORF57 protein (Fig. 1B, red arrow). The expression of HACE1 mRNA in the infected cells was ~2.5-fold higher than the uninfected TIME cells (Fig. 1C). TIVE-LTC cells with latent KSHV genome showed a significant increase in HACE1 expression in the KSHV latency-associated LANA-1 protein expressing cells compared to the uninfected TIVE cells (Fig. 1D, red and white arrows, respectively, and Fig. 1E). A higher level of HACE1 protein was also detected by WB in the TIVE-LTC cells (Fig. 1F). In PEL BCBL-1 cells carrying latent KSHV genome, we observed a significant increase in HACE1 expression compared to that in KSHV-negative BJAB cells both by IFA (Fig. 1G, red and white arrows, respectively) and by WB (Fig. 1H). When we determined the *in vivo* physiological relevance, we observed a significant increase in HACE1 expression in LANA-1-positive KS skin cells compared to healthy skin cells (Fig. 1J, red and white arrows, respectively). A typical phenotypic appearance characteristic of KS lesions is shown in Fig. 1I.

Since a higher level of expression of HACE1 was observed in KSHV-infected cells, we sought to determine the KSHV latent protein responsible for this. We transduced the endothelial cells with lentiviral constructs of KSHV latent ORF71, -72, and -73 and kaposin A genes and observed that kaposin A induced significantly higher expression of HACE1 at both the gene (Fig. 1L) and protein (Fig. 1K) levels than did control (pSIN A) and other latent genes. Together, the increased HACE1 expression in infected cells suggested a potential role of HACE1 in KSHV biology.

HACE1 facilitates resistance to *de novo* KSHV infection-induced oxidative stress. To determine the potential role of HACE1 during KSHV-induced oxidative stress, we knocked down (KD) HACE1 in TIME cells using specific small interfering RNA (siRNA) and the KD efficiency was demonstrated by the >85% reduction in HACE1 protein expression (Fig. 2A). When H_2O_2, an external source of oxidative stress, was added to the HACE1 KD and control TIME cells, HACE1 KD cells were more sensitive and showed a significant level of cell death compared to the control cells (Fig. 2B). To determine the role of HACE1 during KSHV infection-induced oxidative stress, we measured the induction of ROS by IFA using CM-H2DCFDA dye. Increased relative fluorescence intensity demonstrated the KSHV-induced ROS production in the infected cells (Fig. 2C, left column in each set of images, and Fig. 2D). HACE1 KD further resulted in a significant ROS increase over the control cells (Fig. 2C, right column in each set of images, red arrows and white arrows, and Fig. 2D). When ROS induction was measured by fluorescence-activated cell sorting (FACS), we observed an increase in ROS levels in the infected cells which was significantly higher in the HACE1 KD infected cells than in the control cells (Fig. 2E). Supplementation of the antioxidant GSH to the control and HACE1 KD cells minimized the differences in the ROS induction between the two groups of cells compared to their respective counterparts not supplemented with GSH (Fig. 2F). Together, these results suggested that HACE1 plays a protective role in mitigating oxidative stress induced by KSHV infection and that antioxidant elements like GSH can help in maintaining the redox balance.

FIG 1 Legend (Continued)
show increased HACE1 expression in KSHV LANA-1-positive TIVE-LTC cells. (E) Quantitative representation of the relative fluorescence intensity observed in panel D. A minimum of five independent fields, each with at least 10 cells, was chosen. Error bars show SD. ***, $P < 0.001$. (F) HACE1 protein expression in TIVE and TIVE-LTC cells analyzed by WB for HACE1 and β-actin proteins. (G) Immunofluorescence analysis of KSHV-negative BJAB and KSHV-positive BCBL-1 cells by incubation with rabbit anti-HACE1 antibody and then with goat anti-rabbit (Alexa Fluor 488 [green]) secondary antibody. DAPI was used to visualize the nuclei. The white arrows indicate lower expression of HACE1 in the uninfected BJAB cells, and the red arrows indicate increased HACE1 expression in KSHV-positive BCBL-1 cells. (H) HACE1 and β-tubulin protein expression in BJAB and BCBL-1 cells was analyzed by WB. (I) Healthy skin and Kaposi's sarcoma (KS) skin tissue samples were stained by hematoxylin to visualize the cell morphology. (J) A total of five formalin-fixed, paraffin-embedded healthy skin and KS skin tissue samples were first deparaffinized and then rehydrated. The antigen retrieval step was performed, followed by staining for rabbit anti-HACE1 and mouse anti-LANA-1 as described for panel D. DAPI was used to visualize the nuclei. In the representative images, the white arrows indicate lower expression of HACE1 in healthy skin tissue, while the red arrows indicate increased HACE1 expression in KSHV LANA-1-positive KS skin tissue. (K) Endothelial (HMVEC-d) cells were transduced with control lentivirus vector or lentiviruses expressing ORF71, -72, or -73 and kaposin A. After 72 h, WB was done to determine the expression of HACE1 protein. (L) HACE1 gene expression was analyzed by real-time RT-PCR from HMVEC-d cells transduced with indicated lentivirus vectors. Results presented are means ± SD from three independent experiments. **, $P < 0.01$.

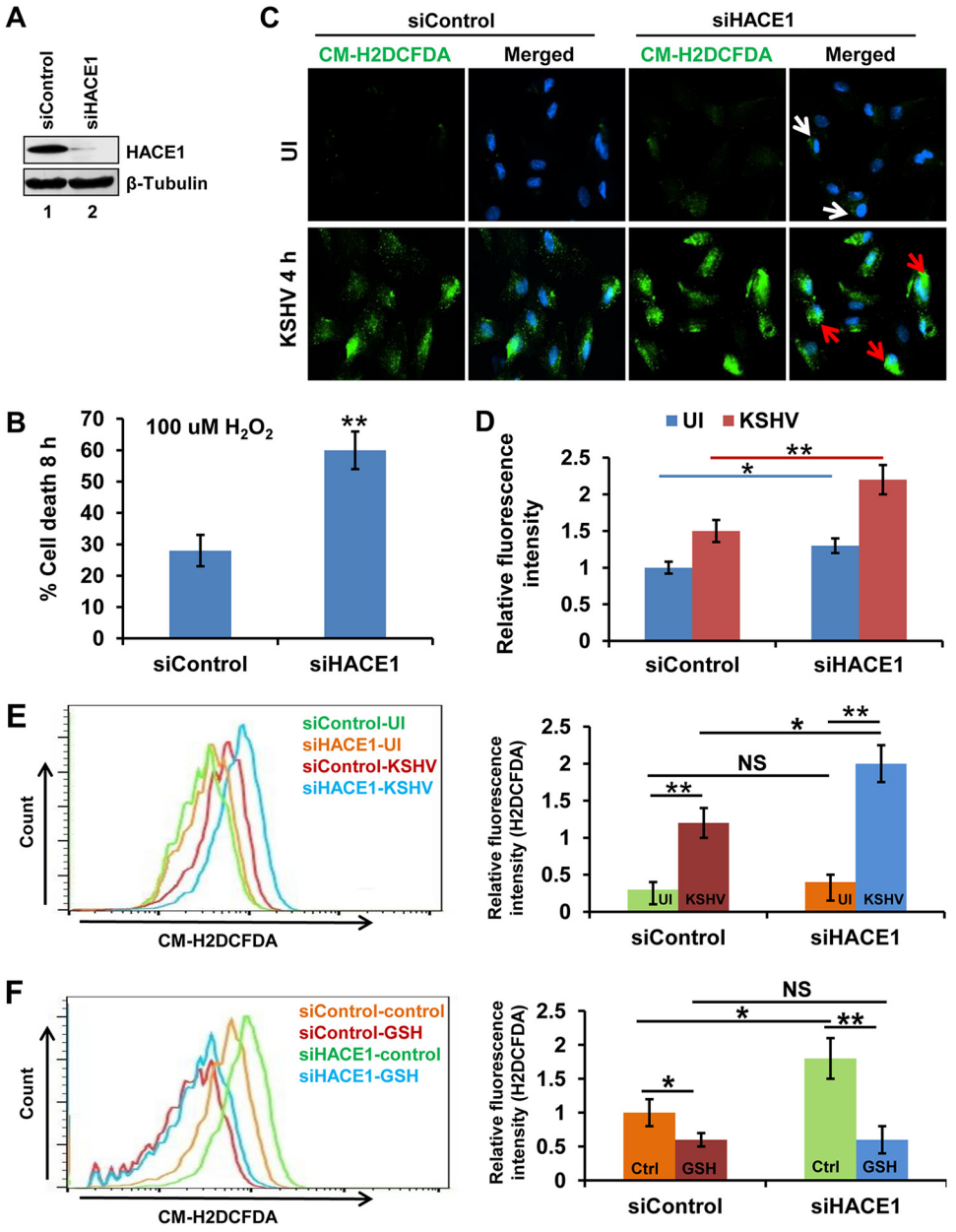

FIG 2 Demonstration of the absence of HACE1 reducing the KSHV infection-induced antioxidative stress response. (A) TIME cells were transfected with siControl or siHACE1 RNA and examined after 48 h by WB for HACE1 and β-tubulin. (B) HACE1 control siRNA or KD TIME cells were treated with H_2O_2 (100 μM) for 8 h and cell death was determined by MTT assay. Results presented are means $\pm$ SD from three independent experiments. **, $P < 0.01$. (C) Immunofluorescence assay analysis of ROS levels in HACE1 wild-type (WT) and KD TIME cells infected with KSHV (30 DNA copies/cell) for 4 h using 2′,7′–dichlorofluorescein diacetate (DCFDA). The white arrows indicate lower detection of ROS in uninfected cells, while the red arrows show increased ROS detection in KSHV-infected cells. (D) Quantitative representation of the relative fluorescence intensity observed in panel C. A minimum of five independent fields, each with at least 10 cells, was chosen. Error bars show SD. *, $P < 0.05$; **, $P < 0.01$. (E) FACS analysis of the ROS levels in HACE1 WT and KD TIME cells infected with KSHV (30 DNA copies/cell) for 4 h by using DCFDA. (Left) Histogram. (Right) relative fluorescence levels ($n = 3$). *, $P < 0.05$; **, $P < 0.01$. NS, not significant. (F) FACS analysis of KSHV-induced ROS levels in HACE1 WT and KD TIME cells treated with GSH (1 μM; 12 h) or untreated controls by using DCFDA. (Left) Histogram. (Right) relative fluorescence levels ($n = 3$). *, $P < 0.05$; **, $P < 0.01$.

Knockdown of HACE1 leads to increase in Rac1 and Nox1 proteins during *de novo* KSHV infection of endothelial cells. HACE1 is known to target the Rac1 protein for proteasomal degradation as a mechanism to balance the Rac1-mediated ROS production by NADPH oxidases (32). Since KSHV also induces ROS and Rac1 (14), we

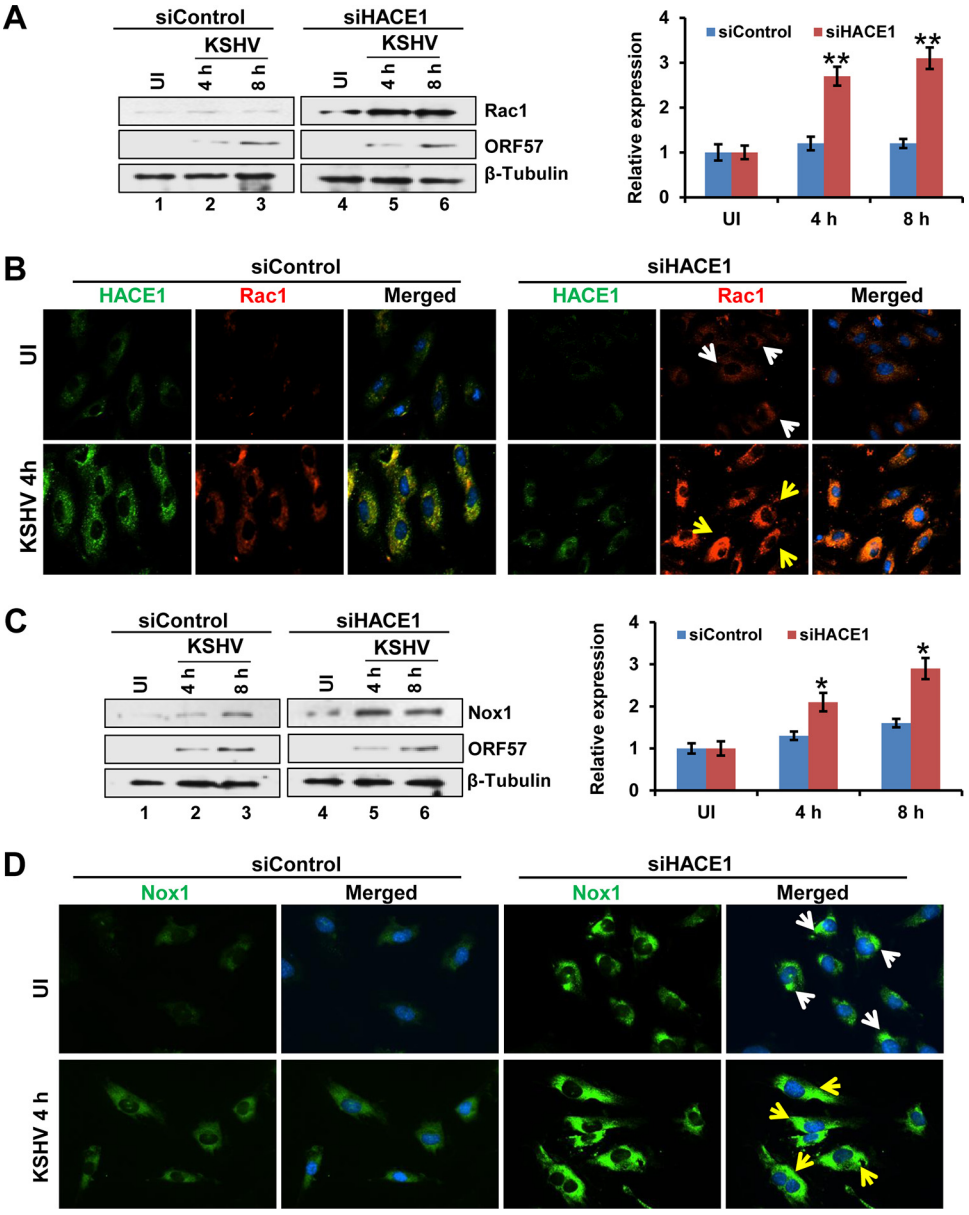

FIG 3 Demonstration of the absence of HACE1 leading into a rise in Rac1 and NADPH oxidase during KSHV infection of endothelial cells. (A and C) TIME cells transfected with siControl or siHACE1 RNA were either left uninfected or infected with KSHV for the indicated times and immunoblotted with anti-Rac1 (A), anti-Nox1 (C), and KSHV IE ORF57 (A and C) antibodies. β-Tubulin was used as a loading control. Fold inductions were normalized to β-tubulin and calculated relative to the uninfected condition, arbitrarily set to 1. The graphs show the statistical significance of the respective WB data. *, $P < 0.05$; **, $P < 0.01$. (B and D) Immunofluorescence analysis of TIME cells with rabbit anti-HACE1 and mouse anti-Rac1 antibody (B) and anti-Nox1 antibody (D) and Alexa Fluor 594 and 488 secondary antibodies. DAPI was used to visualize the nuclei. The white arrows indicate lower expression of Rac1 and Nox1 in uninfected cells, while the yellow arrows show increased Rac1 and Nox1 expression in KSHV-infected cells.

next examined the Rac1 and Nox1 (NADPH oxidase 1) expression during KSHV infection in the absence and presence of HACE1. As we have shown before (14), compared to the control TIME cells, KSHV infection (as measured by the expression of IE ORF57 protein) induced the expression of Rac-1, which was significantly increased and sustained in the HACE1 KD cells (Fig. 3A). KSHV infection led to an overall increase in Rac1 expression as observed by IFA analyses, and the fluorescence intensity observed in the HACE1 KD cells (Fig. 3B, yellow arrows) was significantly higher than in the control cells (Fig. 3B, white arrows). Similarly, a considerable increase in the expression of Nox1 was observed

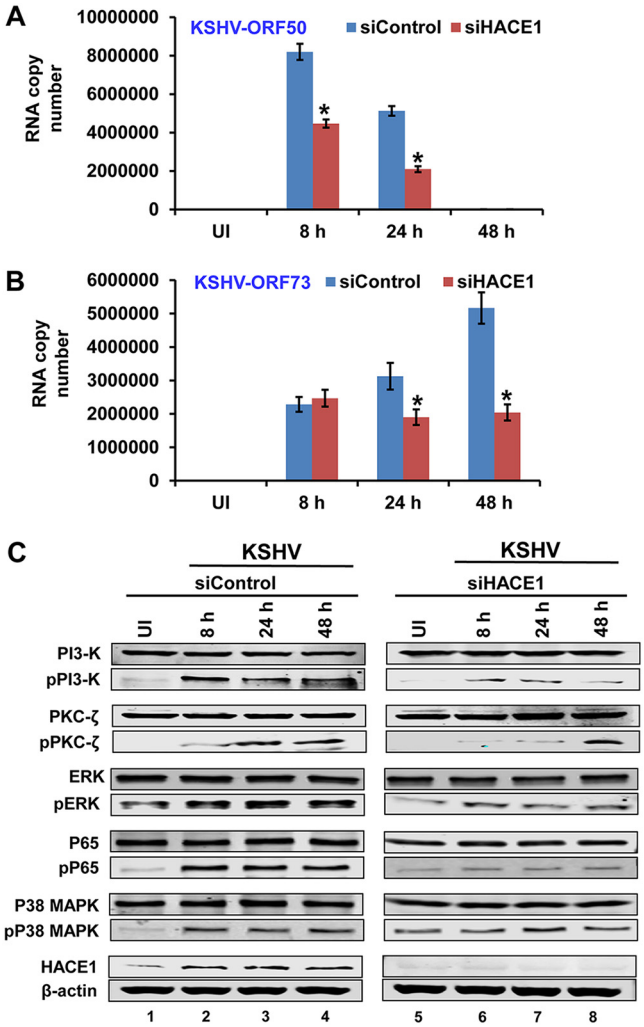

FIG 4 Demonstration of the role of HACE1 in KSHV gene expression. TIME cells transfected with siControl or siHACE1 RNA were either left uninfected or infected with KSHV for the indicated times. (A and B) Total RNA was used in real-time RT-PCR analysis for the KSHV ORF50 and ORF73 genes. Results presented are means ± SD from three independent experiments. *, $P < 0.05$. (C) Western blots of lysates prepared from the cells in panel A with the indicated antibodies. β-Actin was used as a loading control.

during KSHV infection in HACE1 KD cells compared to the control TIME cells both in the WB analysis (Fig. 3C) and in IFA (Fig. 3D, yellow arrows versus white arrows).

Together, these results demonstrated that Rac1 and Nox1 activity increases in the absence of HACE1 and suggested that the absence of HACE1-mediated Rac1 degradation might aid in the overall increase in ROS production during KSHV infection depicted in Fig. 2.

Knockdown of HACE1 leads to a decrease in KSHV gene expression and a decrease in the host cell signal molecules induced during *de novo* KSHV infection. Early during KSHV infection, a limited set of lytic genes are transiently expressed concurrently with the latent genes, leading into the establishment of latent infection (6). Since results in Fig. 1 demonstrated that KSHV infection increased HACE1 expression, which regulates the ROS induction, we next determined the role of HACE1 in viral gene expression. Upon *de novo* KSHV infection of TIME cells, we observed the expression of the lytic switch KSHV ORF50 gene expression at 8 h p.i., which decreased significantly at 24 h p.i. and was not detectable at 48 h p.i. (Fig. 4A). Upon HACE1 KD, ORF50 expression was significantly reduced compared to that in the control cells (Fig. 4A). The expression of KSHV latent ORF73 (LANA-1) gene steadily increased from 8 to

48 h p.i. (Fig. 4B). However, in the HACE1 KD cells, ORF73 expression did not increase after 8 h p.i. and, instead, significantly decreased at 24 and 48 h p.i. (Fig. 4B).

HACE1 deficiency has been shown to impair tumor necrosis factor (TNF)-driven NF-κB activation and apoptosis (36). KSHV *de novo i*nfection induces PI3-K and its downstream targets, such as PKC-ζ, ERK1/2, NF-κB, and p38 MAPK, which are essential for the expression of viral genes and the establishment of latency (16, 26). Moreover, PKC-ζ is essential for the phosphorylation of cytoplasmic Nrf2, which leads to the nuclear translocation of p-Nrf2 and Nrf2-mediated viral and host gene modulation (26). To determine the potential mechanism for the observed reduction in KSHV lytic and latent gene expression in the absence of HACE1, we determined whether HACE1 regulates any of the KSHV infection-induced signal molecules that play roles in viral gene expression. By WB analysis, we observed a significant decrease in the activation of PI3-K, ERK1/2, and NF-κB in HACE1 KD cells compared to that in the control cells (Fig. 4C). PKC-ζ was also significantly reduced compared to the level in control cells until 24 h p.i.; however, not much difference was observed at 48 h p.i. Similarly, p38 MAPK did not show a significant reduction compared to the level in control cells; however, there was a reduction in siHACE1-treated KSHV-infected cells compared to the level in uninfected cells. These results suggested that HACE1 is involved in the amplification of KSHV infection-induced activation of the PI3-K, PKC-ζ, ERK1/2, and NF-κB signal molecules and the consequent KSHV gene expression during *de novo* infection of endothelial cells.

HACE1 regulates Nrf2 translocation from the cytoplasm to the nucleus during *de novo* KSHV infection of endothelial cells. Studies by others and us have shown that Nrf2 phosphorylation leads to its translocation to the nucleus and its transcriptional activity (26, 37). To determine whether HACE1 plays a role in Nrf2 nuclear translocation, we performed cytoplasmic and nuclear protein fractionation of TIME cells followed by WB analysis for the Nrf2 protein. In the nuclear fraction, the Nrf2 levels increased during KSHV infection (Fig. 5A, lanes 9 and 10) compared to the levels in uninfected cells (Fig. 5A, lane 8). In contrast, loss of HACE1 significantly decreased the Nrf2 nuclear translocation levels in both the uninfected and infected cells (Fig. 5A, lanes 11 to 13). Conversely, Nrf2 levels in the cytoplasmic fraction of HACE1 KD cells increased over those in the control cells (Fig. 5A, lanes 1 to 6). By IFA, as demonstrated before (26), there was an enhanced cytoplasmic total Nrf2 (tNrf2) levels and enhanced nuclear phosphorylated Nrf2 (pNrf2) levels in the siControl KSHV-infected cells (Fig. 5B, left sets of images, red arrows) compared to HACE1 KD cells (Fig. 5B), and the pNrf2 predominantly localized in the nuclei of infected cells. In contrast, we observed a significant overall reduction in both tNrf2 throughout the cells and pNrf2 in the nuclei in the HACE1 KD cells (Fig. 5B, white arrows) compared to the control cells (Fig. 5B, red arrows). Real-time reverse transcription-PCR (RT-PCR) analysis with Nrf2-specific primers demonstrated a significant induction of Nrf2 mRNA at 4 and 8 h post-KSHV infection (Fig. 5C, blue bars) compared to HACE1 KD cells (Fig. 5C, red bars). A Western blot from the whole-cell lysate (WCL) prepared from the same batch of cells was performed to show the HACE1 KD cells compared to control cells (Fig. 5D). These results suggested that HACE1 is involved in Nrf2 induction and nuclear translocation in KSHV-infected cells.

HACE1 modulates oxidative stress by promoting Nrf2 activation during *de novo* KSHV infection of endothelial cells. We have shown that Nrf2 levels are significantly increased during KSHV infection of endothelial cells to regulate the expression of several Nrf2 target genes and provide an environment favorable to KSHV infection (26). Since HACE1 loss severely impacted the nuclear translocation of Nrf2, we next determined the effect of HACE1 KD on Nrf2-dependent cellular antioxidant NQO1, COX-2, and HO1 gene expression by real-time RT-PCR at various time points of KSHV infection. The expression levels of NQO1 gene reduced to significantly low levels in the HACE1 KD cells compared to those in the control cells at 4 and 8 h p.i. (Fig. 6A). Similar results were also obtained with HO1, which is involved in heme metabolism (38) (Fig. 6B). COX-2 is important in KSHV infection, which is dependent on Nrf2 induction (17).

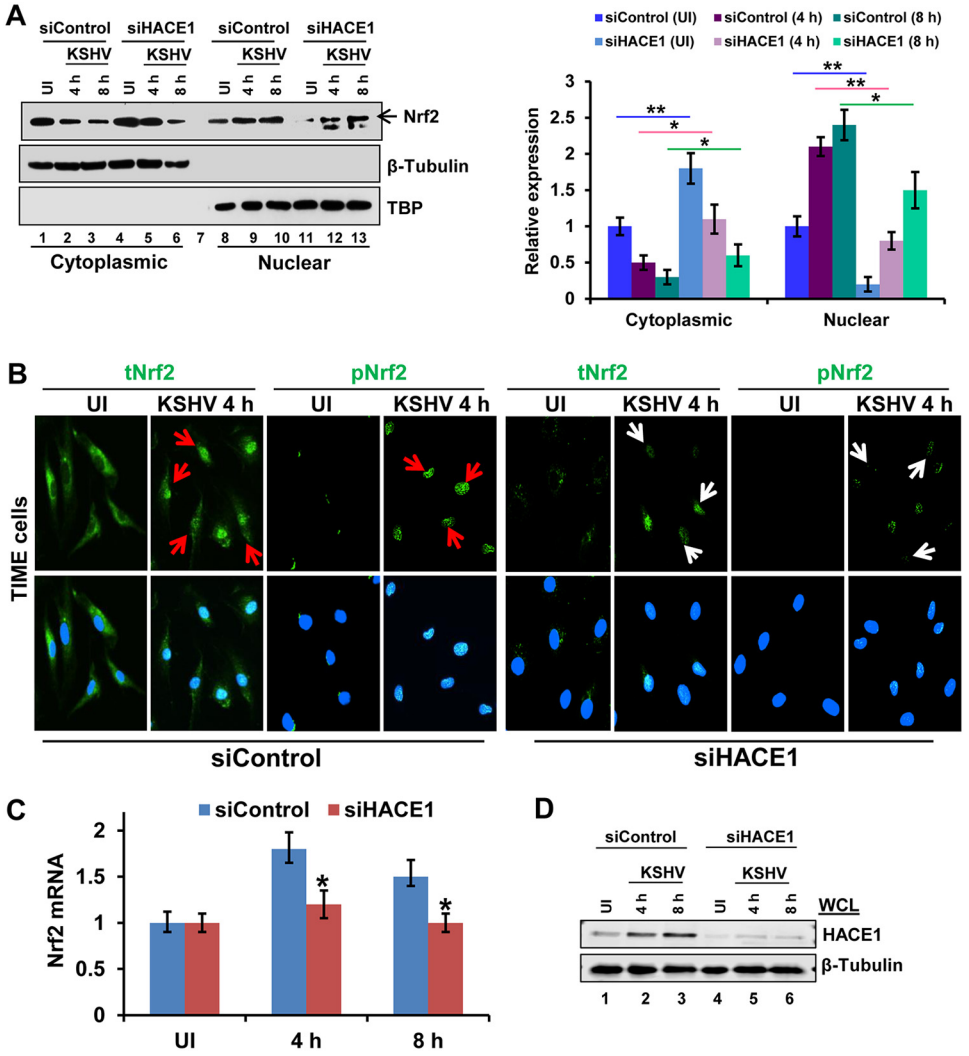

FIG 5 Demonstration of the role of HACE1 in Nfr2 translocation into nucleus during *de novo* KSHV infection-induced oxidative stress. (A) TIME cells transfected with siControl or siHACE1 RNA were either left uninfected or infected with KSHV for the indicated times. Cells were lysed and fractionated to isolate nuclear and cytosolic fractions, and fractions were confirmed by WB with β-tubulin as a marker for cytosolic fractions and TATA binding protein (TBP) as a marker for nuclear fractions. Nrf2 nuclear localization was determined using anti-Nrf2 antibodies and quantified relative to TBP. The graph shows the statistical significance of WB data. *, $P < 0.05$; **, $P < 0.01$. (B) Nrf2 localization and levels during KSHV infection (30 DNA copies/cell) were visualized by IFA. Serum-starved cells were infected with KSHV for 4 h and stained for tNrf2 and pNrf2 in both WT and HACE1 KD TIME cells. DAPI was used to visualize the nuclei. Red arrows indicate the normal localized expression of tNrf2 and pNrf2 in control cells, while the white arrows indicate an overall reduction in the translocation of both tNrf2 and pNrf2 in the nuclei of siHACE1 RNA-treated cells. (C) Real-time RT-PCR analysis of Nrf2 mRNA measured at various times after infection of TIME cells transfected with siControl and siHACE1 RNA. Each point represents fold induction compared to that for uninfected cells (arbitrarily set to 1) $\pm$ SD for 3 independent experiments. *, $P < 0.05$. (D) Western blotting from the WCL prepared from the same batch of cells was performed to show a representative KD of HACE1 compared to control cells.

We observed a significant decrease in the expression of COX-2 mRNA in HACE1 KD cells compared to that in control cells (Fig. 6C). To determine if the mRNA expression corroborated the protein expression levels, we performed WBs for the NQO1 and COX-2 proteins. Significant increases in the expression of HACE1 (3.6-fold) and Nrf2 downstream NQO1 (16-fold) and COX-2 (19-fold) proteins were observed during KSHV infection as measured by IE ORF57 expression (Fig. 6D); these were significantly reduced by HACE1 KD (Fig. 6E). IFA results were also consistent with the WB data and showed significantly reduced expression of both NQO1 (Fig. 6F) and COX-2 (Fig. 6G) in HACE1 KD KSHV-infected cells compared to control KSHV-infected cells. Collectively,

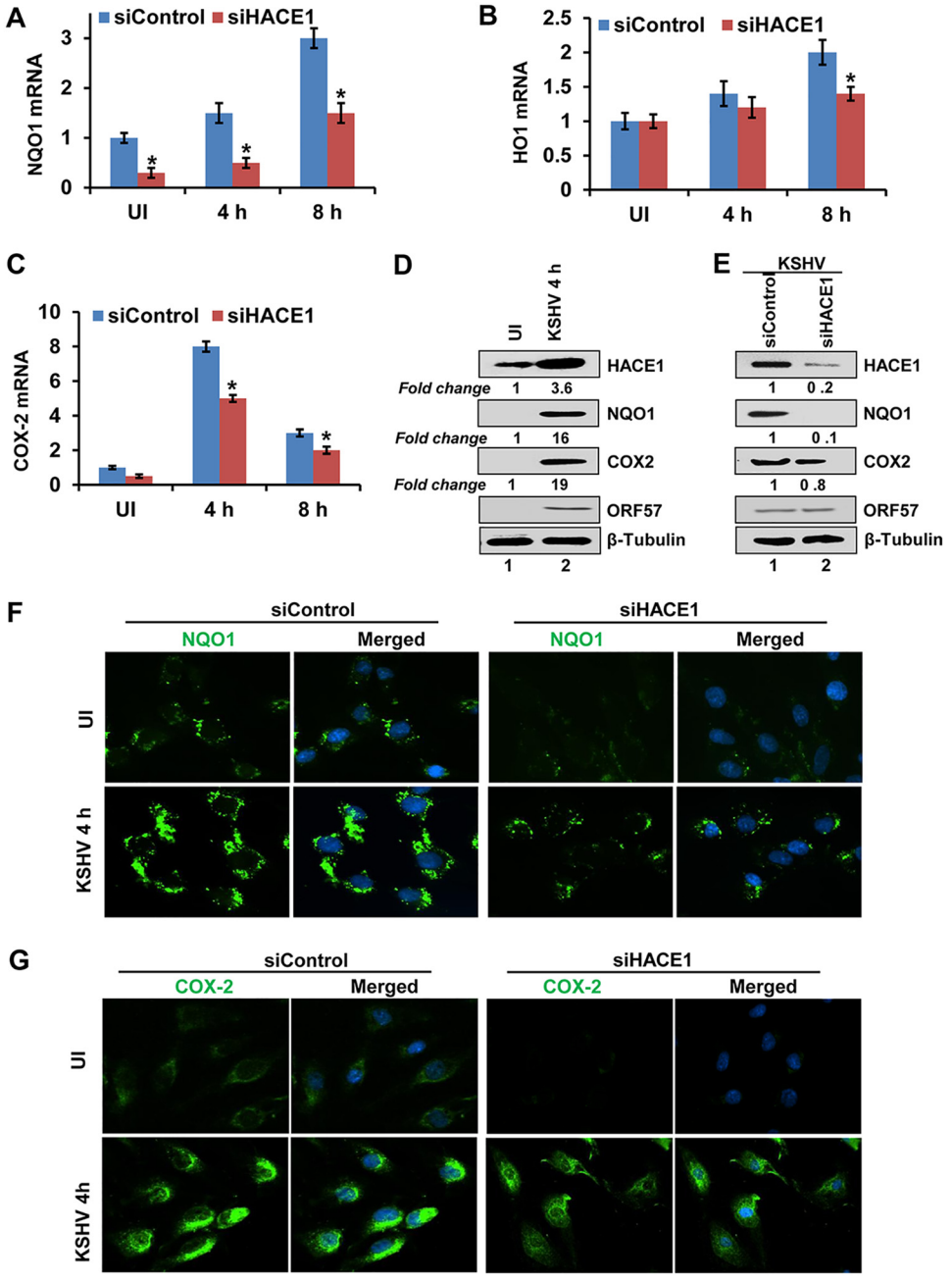

FIG 6 Demonstration of HACE1 promoting Nrf2 activities during KSHV infection. (A, B, and C) TIME cells transfected with siControl or siHACE1 RNA were either left uninfected or infected with KSHV for the indicated times and analyzed by real-time RT-PCR for the Nrf2 target genes (NQO1, COX-2, and HO1 genes) involved in ROS homeostasis. The UI siControl cells were arbitrarily set to 1, and the bars indicate mean fold induction ± SD for 3 independent experiments. *, $P < 0.05$. (D and E) WB analysis. (D) Fold change in HACE1, NQO1, and COX-2 proteins induction upon KSHV infection (indicated by IE ORF57 expression). (E) Fold change in HACE1, NQO1, and COX-2 proteins induction upon KSHV infection in siControl and siHACE1 RNA-transfected TIME cells. β-Tubulin was used as the loading control. (F and G) Immunofluorescence analysis of the expression of Nrf2 target COX-2 and NQO1 proteins in siControl and siHACE1 RNA-transfected TIME cells upon KSHV infection.

these results suggested that HACE1 is required for optimal Nrf2 activation in response to KSHV-induced oxidative stress and for modulation of antioxidative stress response genes and other vital genes that are induced in an Nrf2-dependent manner during KSHV infection.

HACE1 promotes Nrf2 activation during *de novo* KSHV infection of endothelial cells. Our previous studies have shown that Nrf2 plays a crucial role during KSHV-

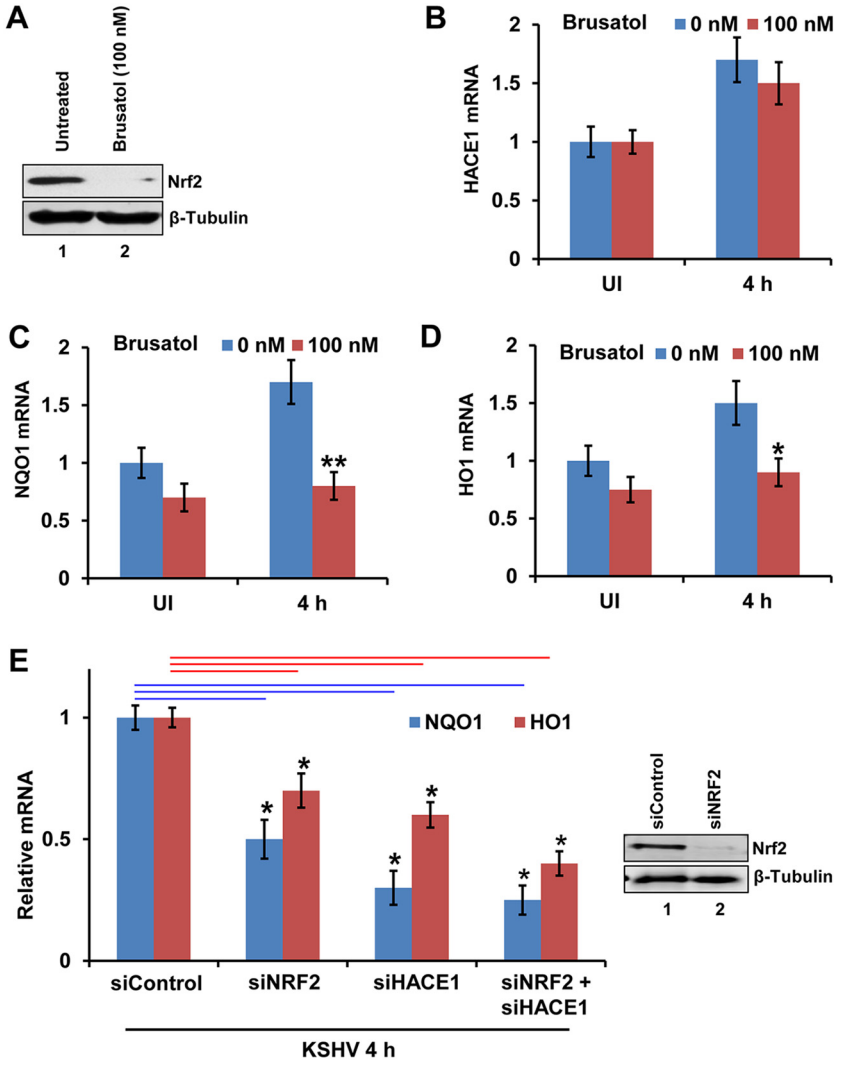

FIG 7 Demonstration of HACE1 promoting Nrf2 activity to cope with KSHV-induced oxidative stress. (A) TIME cells treated with 100 nM brusatol for 8 h were tested by WB for Nrf2 protein expression. (B, C, and D) Brusatol-treated uninfected and KSHV-infected cells were analyzed by real-time RT-PCR for the HACE1, NQO1, and HO1 mRNA expression. (E) TIME cells were transfected with control siRNA, siNrf2, siHACE1, or combined siNrf2+HACE1 RNA and analyzed by real-time RT-PCR for NQO1 and HO1 mRNA expression. Results presented are means ± SD from three independent experiments. *, $P < 0.05$; **, $P < 0.01$. The WB on the right side of panel E shows the representative KD condition of Nrf2 in the cells.

induced oxidative stress (26), and a recent study demonstrated the potential role of the HACE1 gene as an oxidative stress response gene (33). We thus examined whether HACE1 by itself can act as an independent player in the antioxidant response in the absence of Nrf2. For this, we used Brusatol, a chemical inhibitor of Nrf2 that mediates the proteasomal degradation of Nrf2 (39). We used Brusatol at a 100 nM concentration, as this has been shown to significantly reduce the expression of Nrf2 without affecting the viability of uninfected endothelial cells (28). The effects of Brusatol on Nrf2 protein can be seen in the WB of TIME cells (Fig. 7A). Brusatol did not affect the expression of HACE1 mRNA in the absence of Nrf2 (Fig. 7B) in KSHV-infected cells, which indicated that Nrf2 acts as a downstream molecule and may not regulate the expression of HACE1. However, an increase in expression of HACE1 in Brusatol-treated KSHV-infected cells compared to the uninfected cells (Fig. 7B), even in the absence of Nrf2, showed that HACE1 probably acts as an independent oxidative stress response mediator. Next we determined whether HACE1 regulates the Nrf2 downstream molecules in the absence of Nrf2. As seen before, NQO1 (Fig. 7C) and HO1 (Fig. 7D) gene expression

increased during infection, which was blocked significantly by the Brusatol treatment. However, there was a slight increase in the expression of both the NQO1 and HO1 genes in the infected cells compared to the uninfected cells even in the absence of Nrf2 (Fig. 7C and D), which indicated a possible role of HACE1 in directly regulating NQO1 and HO1 expression or indirect regulation by Nrf2 or via another potential player(s) of redox control. This suggestion was further strengthened by the analysis of various KD conditions with siNrf2, siHACE1, and siNrf2 plus siHACE1 in the infected cells. The double KD of Nrf2 and HACE1 showed the maximum reduction in the NQO1 and HO1 gene expression compared to their individual KD effects (Fig. 7E). The WB on the right side of Fig. 7E shows the representative KD condition of Nrf2 in the cells. These results suggested that HACE1 acts as an oxidative stress response mediator predominantly by promoting the Nrf2 activity and further strengthen our findings of HACE1 being a key player during KSHV-induced oxidative stress.

Loss of HACE1 leads to ROS-dependent increased glutamine uptake in endothelial cells latently infected with KSHV. Glutamine plays an important role during oxidative stress, as it is metabolized to generate NADPH and glutamate, which is required for the synthesis of antioxidant glutathione (40). Increased glutamate secretion and glutaminase expression were observed in KSHV *de novo*-infected endothelial cells as well as in KSHV latently infected endothelial and B cells (41). Latent KSHV infection led to increased levels of intracellular glutamine and enhanced glutamine uptake, and further depletion of glutamine in culture medium led to cellular apoptosis (42). A study showed that in the absence of HACE1, glutamine uptake was increased to balance the increased ROS levels (43). Hence, we next determined whether HACE1 KD affects the glutamine uptake to cope with the oxidative stress in KSHV-infected cells. To determine whether glutamine is required for the survival of KSHV latently infected endothelial cells, we treated TIME cells with glutamine-replete or glutamine-free medium and the percent cell death was determined at 24 and 48 h posttreatment. KSHV-infected cells supplemented with glutamine-replete medium showed a higher percentage of cell death, which increased drastically in the virus-infected cells deprived of glutamine (Fig. 8A). To our surprise, the percent cell death further increased, to ~35%, in KSHV-infected (48 h p.i.) HACE1 KD cells in glutamine-deprived medium compared to the KSHV-infected (48 h p.i.) HACE1 KD cells in the glutamine-replete medium (Fig. 8B). Increased cell death under the HACE1 KD glutamine-starved condition compared to control cells was also demonstrated by ethidium homodimer 1 staining (Fig. 8B). When we performed a glutamine uptake assay in the control versus HACE1 KD cells upon KSHV infection, we observed a gradual increase in the glutamine uptake during 24 and 48 h p.i. compared to that in the uninfected cells. An overall increase at all time points was observed in the HACE1 KD cells compared to their control counterparts (Fig. 8C). These results demonstrated that endothelial cells require HACE1 to cope with oxidative stress induced during KSHV infection and that this event require the increased level of glutamine during prolonged viral infection.

DISCUSSION

Our comprehensive studies presented here demonstrate that HACE1, an E3 ligase protein, plays an important role in the regulation of KSHV-induced oxidative stress by promoting Nrf2 activity in endothelial cells. Higher expression of HACE1 during *de novo* infection of endothelial cells, in KSHV latently infected TIVE-LTC and BCBL-1 cells as well as in the KS tissues, suggests that HACE1 is important for the biology of KSHV. Earlier studies have shown the crucial roles of several KSHV latent proteins in regulating cellular processes to make the environment conducive to viral infection (26, 41, 44). We have previously shown that kaposin A, which is one of the proteins expressed during KSHV latency, played crucial roles in KSHV-induced cell proliferation by activating metabotropic glutamate receptor 1 (mGluR1) during KSHV infection (41). Kaposin A has also been shown to mediate oncogenesis *in vitro* in Rat3 fibroblasts and in nude mice (45, 46). Another study by Kliche et al. demonstrated the mechanistic role of kaposin A in the oncogenic transformation of NIH 3T3 fibroblasts (47). Similar to these findings,

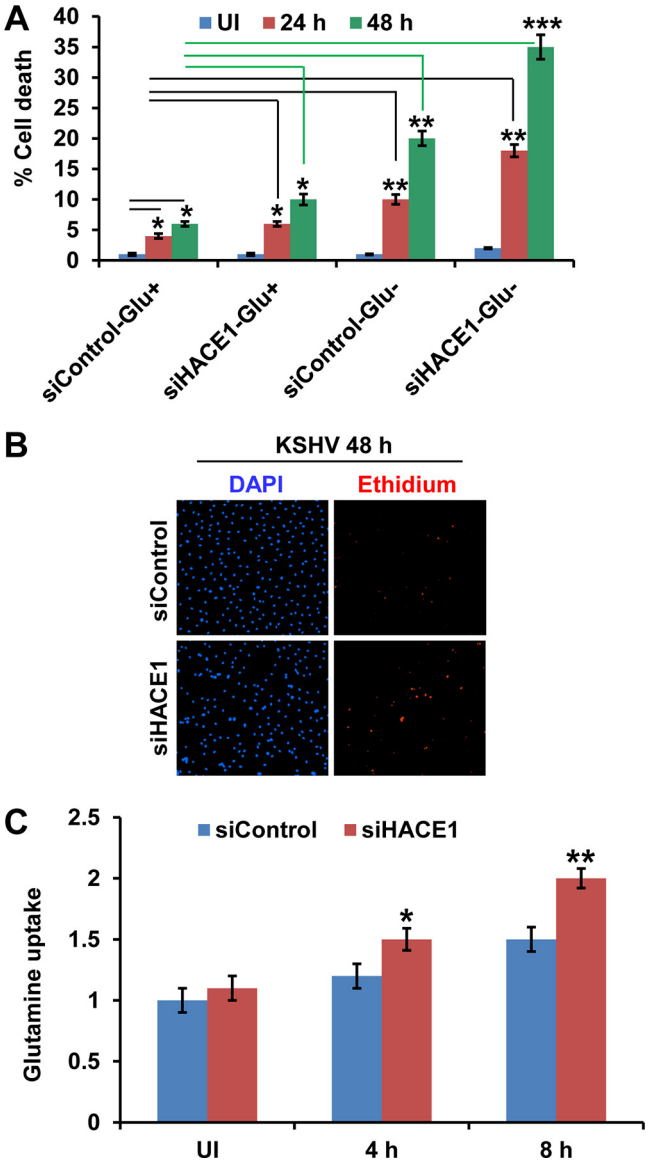

FIG 8 Demonstration of the loss of HACE1 leads to increased glutamine requirement of endothelial cells to manage KSHV-induced oxidative stress. (A) TIME cells transfected with control siRNA and siHACE1 RNA were either left uninfected or KSHV infected and treated with replete or glutamine-free medium. Cell death was analyzed at 24 and 48 h posttreatment by MTT assay. Results presented are means ± SD from three independent experiments. *, $P < 0.05$; **, $P < 0.01$. (B) Representative image of the ethidium homodimer 1-stained WT and HACE1 KD TIME cells after 48 h of glutamine starvation (48 h p.i.) from panel B. (C) HACE1 KD TIME cells take up more glutamine (Gln) than WT cells. Uninfected and KSHV-infected HACE1 KD and control TIME cells were incubated in Gln-free medium for 1 h, followed by the addition of glutamine. The fold change in Gln uptake was determined using a commercially available glutamine uptake assay kit as per the manufacturer's instructions. Cells were incubated in Gln-free medium for 1 h, followed by addition of glutamine. *, $P < 0.05$; **, $P < 0.01$.

our current study also indicates a potential role of kaposin A in the enhanced expression of HACE1 (Fig. 1).

ROS are produced as a natural by-product of normal metabolism of oxygen, an inexorable consequence required for cellular homeostasis (48, 49). Under normal nonpathogenic conditions, ROS are known to play crucial roles in several cellular processes, such as differentiation, proliferation, and cell motility (50). However, under pathogenic conditions, including viral infections, ROS have been reported to oxidize DNA, causing damage and posing a threat to the cellular integrity (51). Several viruses utilize ROS (52), and studies with KSHV latently infected endothelial cells have dem-

onstrated the role of ROS in lytic reactivation of KSHV (10, 11, 53). Studies have also shown the downstream effects of ROS activation during KSHV infection (26–28). KSHV infection also induces ROS in the endothelial cells to facilitate its entry and to amplify the infection-induced initial host cell signaling cascade (54). In addition to mitochondria, which mainly produce ROS during oxidative phosphorylation events (55), NADPH oxidases are a major source of cellular ROS (56). Since ROS are known to have damaging effects on the cellular integrity (57), a tightly regulated cellular response is always active to balance the excess oxidative stress. One such master regulator of cellular antioxidative stress response is Nrf2, which is one of the downstream targets of ROS. Nrf2 has been shown to be activated by several viruses (58, 59), including KSHV (26–28).

Our previous studies have demonstrated that KSHV infection induces the activation of Nrf2, which subsequently translocates to the nucleus to induce the host antioxidative response genes, as well as host and viral genes that are required for successful infection and establishment of latency (Fig. 9) (26). Studies have shown that HACE1 has a protective role against stress-induced tumorigenesis in mice (60, 61). A study further showed that HACE1 plays crucial roles in the Nrf2 antioxidative stress response pathway and was observed to be in reduced levels in Huntington disease leading to neurodegeneration (33). HACE1 protects the cells from mutant Huntingtin toxicity by augmenting the Nrf2 response (33). Similar to these studies, we also observed a protective role of HACE1 during oxidative stress from an external source (H_2O_2) and during KSHV infection of endothelial cells. The absence of HACE1 significantly increased cell death upon oxidative stress, while this was restored upon external supplementation of glutathione (an antioxidant). Studies with vertebrates have shown that HACE1 targets Rac1 when it is bound to NADPH oxidase holoenzyme, thus blocking the generation of ROS by Rac1-dependent NADPH oxidases and conferring cellular protection against ROS-induced DNA damage and cyclin D1-driven hyperproliferation (32). Similar to these findings, our studies also demonstrate elevated expressions of both Rac1 and Nox1 during KSHV infection and these expressions were further enhanced in HACE1 knockdown cells, showing the role of HACE1 in the management of ROS during KSHV infection (Fig. 9).

KSHV has evolved to utilize several key host proteins in its favor, and several host factors are utilized by KSHV during entry, trafficking, nuclear delivery of the viral genome, and establishment of latency (15, 16, 26, 62). In our current study we observed a direct correlation of HACE1 to KSHV gene expression. The silencing of HACE1 significantly reduced ORF50 expression compared to that in the control cells. This effect was also drastically enhanced in ORF73 expression: control cells showed an increase in ORF73 expression, while the HACE1 KD cells demonstrated a significant decrease in the expression, thereby hampering viral latency (Fig. 4A and B). Interestingly, ORF73 expression was induced at 8 h p.i. in both control and HACE1 KD cells, thereby raising the possibility that HACE1 might not be the only factor in play; future studies are required to understand the exact mechanism. Our studies have shown that PKC-ζ is essential for the activation of Nrf2 and its subsequent translocation into the nucleus to enhance Nrf2-mediated gene expression during KSHV infection (26). A significant reduction observed in the translocation of Nrf2 from the cytoplasm to nuclei of KSHV-infected HACE1 KD cells can be directly attributed to the reduction of PKC-ζ activation in the HACE1 KD cells. Reduction in Nrf2 translocation in the absence of HACE1 also affected the downstream Nrf2 target NQO1, HO1, and COX-2 genes, thus contributing the absence of antioxidative response in the HACE1 KD cells. Although we observed a significant decrease in the expression of NQO1, HO1, and COX-2 genes in the absence of Nrf2 activity in KSHV-infected cells, there was a slight increase in these genes in the presence of HACE1, which suggested that HACE1 could also have an independent function potentially involving other transcription factors (63).

We have shown previously that KSHV *de novo i*nfection induces PI3-K and its downstream PKC-ζ, ERK1/2, NF-κB, and Nrf2 targets, which are essential for the expression of viral genes and the establishment of latency (16, 26), and PKC-ζ is essential for Nrf2 phosphorylation, nuclear translocation of pNrf2, and Nrf2-mediated viral and host

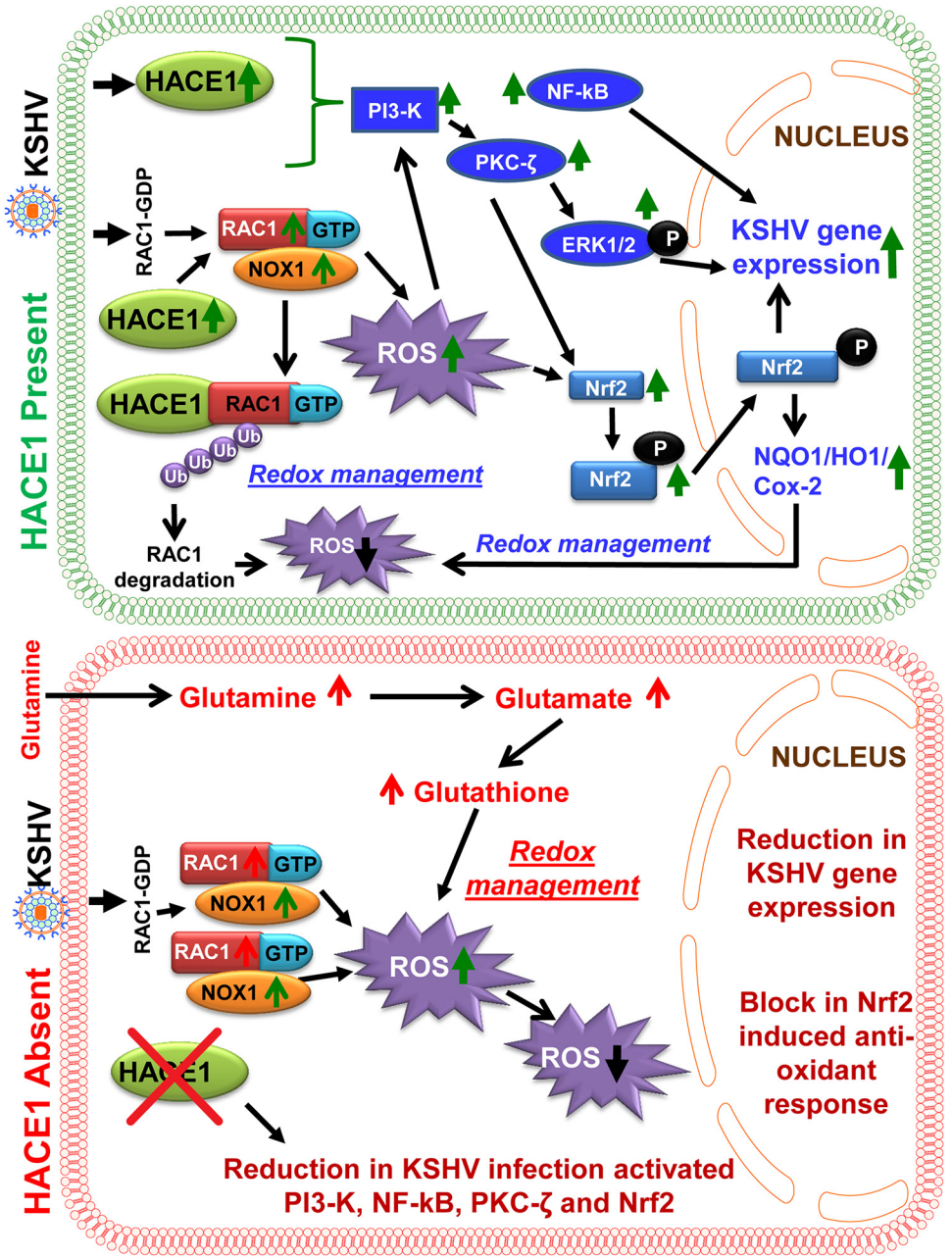

FIG 9 Schematic of the role of HACE1 during KSHV infection of endothelial cells. HACE1 plays crucial roles in the management of oxidative stress. (Upper portion, green) HACE1, under normal nonpathogenic conditions, targets Rac1 for proteasomal degradation, thus reducing ROS levels. Under pathogenic conditions such as KSHV infection, the activity of HACE1 increases, leading to the enhancement of the virus-induced signaling cascade (PI3-K, PKC-ζ, ERK1/2, NF-κB, and p38 MAPK), which results in the activation of Nrf2, nuclear translocation of pNrf2, and Nrf2-mediated viral and host gene modulation as well as redox management. (Lower portion, red) In the absence of HACE1, the activity of Rac1 increases significantly, leading to a higher level of ROS. Cells take up more glutamine in order to synthesize more GSH for redox management. The loss of HACE1 also reduces KSHV-induced expression of PI3-K, PKC-ζ, ERK1/2, NF-κB, p38 MAPK, and Nrf2, and, consequently, the expression of viral genes during *de novo* KSHV infection of endothelial cells.

gene modulation (26). Reduction in PI3-K, PKC-ζ, ERK1/2, and NF-κB activation and loss of nuclear translocation of Nrf2 in the absence of HACE1 demonstrated that HACE1 plays a role in KSHV gene expression via the amplification of infection-induced PI3-K, PKC-ζ, ERK1/2, and NF-κB activation and by aiding in the nuclear translocation of Nrf2 (Fig. 9). Whether HACE1 amplifies these signal molecules via its E3 ligase activity is not known at present and needs further study.

Glutamine is required by many cancer cells for their survival. Studies demonstrate that KSHV has evolved to exploit the cellular metabolism for its survival and maintenance of latently infected cells and to require glutamine for anabolic proliferation of KSHV-transformed cells (64, 65) and maintenance of endothelial cells latently infected with KSHV (42). Loss of HACE1 has been linked with ROS-dependent increased glutamine uptake in mouse embryonic fibroblasts (43). The cells deficient in HACE1 showed uncontrolled production of ROS and the cell death was enhanced further upon glutamine withdrawal. While glutamine starvation increased the ROS levels, external supplementation of the antioxidant *N*-acetylcysteine (NAC) restored the ROS levels (43). Glutamine metabolism generates NADPH and glutamate is required for synthesis of the antioxidant glutathione (GSH), which contributes to redox balance in transformed cells. Increased glutamate secretion and glutaminase expression in KSHV *de novo*-infected endothelial cells and in KSHV latently infected endothelial and B cells (41) correlate with our findings here and demonstrate the requirement of glutamine in KSHV-infected cells to cope with the increased ROS-induced oxidative stress and for the survival of latently infected cells.

In summary, our findings demonstrate an essential role of HACE1 in mitigating KSHV-induced oxidative stress, and this event is predominately mediated by the facilitation of Nrf2 function. These results provide strong evidence that HACE1 can be targeted therapeutically to manage KSHV infections and pathogenesis.

MATERIALS AND METHODS

Cells. KSHV-negative BJAB and KSHV-positive BCBL-1 cells with >80 copies of latent KSHV genomes/cell were cultured in RPMI 1640 GlutaMax (Gibco Life Technologies, Grand Island, NY) supplemented with 10% (vol/vol) fetal bovine serum (FBS; HyClone, Logan, UT) and 1% penicillin-streptomycin (Gibco) (2). hTERT-immortalized microvascular endothelial (TIME) cells (1) (Lonza, Walkersville, MD) were maintained as monolayer cultures in endothelial cell growth medium (ATCC, Manassas, VA) supplemented with a bullet kit containing all required growth factors. The telomerase-immortalized human umbilical vein endothelial (TIVE) cells and long-term-KSHV-infected TIVE cells (TIVE-LTC cells), generous gifts from Rolf Renne (University of Florida, Gainesville, FL), were cultured in endothelial basal medium 2 (EBM-2) with growth factors (Lonza). Human dermal microvascular endothelial cells (HMVEC-d-CC-2543; Lonza) were cultured in EBM-2 supplemented with the EGM-2MV BulletKit (Lonza). Growth medium with dialyzed FBS and depleted of glucose, glutamine, and other small molecules was used for all experiments that required glutamine-free medium. All cells were regularly tested and confirmed to be mycoplasma negative using the Mycoalert kit (Lonza).

Virus. The lytic cycle of KSHV was induced in BCBL-1 cells by treatment with 20 ng/ml of 12-*O*-tetradecanoyl-phorbol-13-acetate (TPA; Millipore Sigma, Billerica, MA), followed by supernatant collection and virus purification as per procedures described previously (66). DNA was extracted from purified KSHV, and viral copy numbers were estimated by real-time DNA-PCR using TaqMan primers and probes for the KSHV ORF73 gene as described previously (6). The same batch of purified KSHV at 30 DNA copies/cell (multiplicity of infection [MOI]), unless stated otherwise, was used for all the experiments. All cells were regularly tested and confirmed to be mycoplasma negative using the Mycoalert kit (Lonza). Infection rates were assessed by performing an immunofluorescence assay for KSHV LANA-1 expression (66).

Reagents. H_2O_2 and glutathione (GSH) were from Sigma. The CM-H2CDFDA ROS-measuring dye was from Life Technologies, Thermo-Fisher Scientific, Carlsbad, CA. The nuclear extract kit was from Active Motif, Carlsbad, CA. The glutamine assay kit was from BioVision, Mountain View, CA.

Antibodies. Mouse monoclonal anti-LANA-1 antibody 1D10C3 (IgG1) was generated in our laboratory against the LANA-1 ORF amino acid sequence CEPQQREPQQREPQQ conjugated with keyhole limpet hemocyanin (KLH). Rabbit anti-ORF57 was from Boster Biological Technology, Pleasanton, CA. Mouse monoclonal antibodies against HACE1, Nrf2, NQO1, and COX-2 were from Santa Cruz Biotechnology, Inc., Santa Cruz, CA. Rabbit monoclonal antibodies against HACE1, pNrf2, and Nox1 were from Abcam, Boston, MA. Anti-Rac1 antibodies were from BD Biosciences, San Diego, CA. Anti-phospho-PKC-ζ (anti-p-PKC-ζ), PKC-ζ, p-PI3-K, PI3-K, p-ERK, ERK, p-p65, p65, p-p38 MAPK, and p38 MAPK antibodies were from Cell Signaling Technology, Beverly, MA. 4′,6-Diamidino-2-phenylindole (DAPI) and Alexa Fluor 488 and 594 (rabbit or mouse) were from Molecular Probes, Invitrogen, Carlsbad, CA. Anti-β-actin, β-tubulin, and TATA binding protein (TBP) antibodies were from Sigma.

Lentivirus transduction. Lentiviral constructs for KSHV ORF71 (vFLIP), ORF72 (vCyclin), ORF73 (LANA-1), and ORFK12 (kaposin A) were a gift from Chris Boshoff at the UCL Cancer Institute. These were utilized for lentivirus production and transduction as described previously (41, 67).

siRNA transfection. A pool of 3 target-specific siRNA oligonucleotides against HACE1 were purchased from Santa Cruz Biotechnology, Inc. TIME cells were transfected with target-specific siRNA using the Neon transfection system (Invitrogen) according to the manufacturer's instructions. Briefly, subconfluent cells were harvested from the culture flasks, washed once with 1× phosphate-buffered saline (PBS), and resuspended in resuspension buffer R (Invitrogen). The cell suspension was gently mixed with

200 pmol of control or target-specific siRNA and then microporated at room temperature using a single pulse of 1,350 V for 30 ms. After microporation, cells were distributed into prewarmed complete medium and placed at 37°C in a humidified 5% CO_2 incubator. At 48 h posttransfection, the cells were analyzed for knockdown efficiency by Western blotting.

Cell fractionation and Western blotting. Cells were lysed in radioimmunoprecipitation assay (RIPA) lysis buffer (15 mM NaCl, 1 mM $MgCl_2$, 1 mM $MnCl_2$, 2 mM phenylmethylsulfonyl fluoride, and protease inhibitor mixture [Sigma]), and protein concentration estimation was performed using the bicinchoninic acid (BCA) protein assay reagent (Pierce, Rockford, IL) according to the manufacturer's instructions. Equal concentrations of proteins were separated by subjecting to SDS-PAGE on a 4 to 15% Mini-PROTEAN gel (Bio-Rad). The proteins were transferred to a 2.2-μm nitrocellulose membrane (Bio-Rad) and blocked with 5% nonfat dry milk in Tris-buffered saline (TBS) with 0.1% Tween (TBST) for 1 h. The membranes were then probed with the appropriate specific primary antibodies, followed by incubation with species-specific horseradish peroxidase (HRP)-conjugated secondary antibody. The immunoreactive protein bands were detected by chemiluminescence-based detection (Pierce) method as per the manufacturer's protocol and processed in an autoprocessor. The bands were scanned using the FluorChem FC2 and Alpha-Imager systems (Alpha Innotech Corporation, San Leonardo, CA), and densitometry measurements were made using ImageJ software (NIH).

To analyze the intracellular distribution of Nrf2, TIME cells were infected with KSHV at different time points and the nuclear and cytoplasmic protein fractions were obtained using a commercially available kit (Active Motif) following the manufacturer's instructions. Briefly, the cells were trypsinized and washed twice with PBS having a phosphatase inhibitor followed by cell lysis using 1× hypotonic buffer to disrupt the plasma membrane. The lysate was centrifuged at 14,000 × *g* for 30 s to pellet the nuclei and collect the cytoplasmic fraction. The nuclear pellet was washed twice with 1× hypotonic buffer to remove any loosely bound cytoplasmic contaminants, and the nuclear pellet was finally resuspended in complete lysis buffer to obtain the pure nuclear protein fraction.

ROS measurement. TIME cells were treated with control and HACE1 siRNAs and infected with KSHV for the desired times to analyze the ROS levels as described previously (14). The ROS detecting dye 5 (and 6)-chlormethyl-2′,7′-dichlorohydrofluorescein diacetate, acetyl ester (CM-H2DCFDA [C6827]; Invitrogen) was added to cells for 30 min prior to KSHV infection. ROS were analyzed using fluorescence microscopy and a FACS LSRII flow cytometer (Becton, Dickinson) and FlowJo software.

Glutamine starvation and glutamine uptake assay. The control as well as HACE1 knockdown TIME cells, either left uninfected or infected with KSHV, were seeded into 24-well plates. After infection, the cells were treated with replete medium (4 mM glutamine) and glutamine-free medium in triplicates. A 3-(4,5-dimethyl-2-thiazolyl)-2,5-diphenyl-2H-tetrazolium bromide (MTT) assay was performed at 24 and 48 h p.i. to analyze the cell viability as per the manufacturer's instructions (ATCC). The glutamine uptake assay was performed using a commercially available glutamine colorimetric assay kit (BioVision) following the manufacturer's instructions. Briefly, the control as well as siHACE1-treated TIME cells were either left uninfected of KSHV infected for the desired times in a 96-well plate. The cells were incubated with glutamine-free medium for 1 h prior to desired time points and washed 3 times with PBS, followed by the addition of 1 mmol/liter of glutamine. The glutamine concentration was determined by comparing the readings of test samples, after subtracting the background signal, with a standard curve. The readings were obtained by measuring the absorbance (optical density [OD] at 450 nm) in a plate reader (BioTek, Winooski, VT).

qRT-PCR. KSHV gene expression was assessed by extracting the total RNA from KSHV-infected cells using an RNeasy minikit (Qiagen) followed by one-step quantitative real-time RT-PCR (qRT-PCR) analysis using ORF50 and ORF73 gene-specific primers and TaqMan probes as described previously (6, 66). The absolute copy number calculation of each mRNA was done using the standard curves specific for ORF50 and ORF73, obtained from *in vitro*-derived transcripts as described previously (6). Host gene expression was also analyzed by extraction of total RNA followed by reverse transcription to create the cDNA library and subsequent performance of a real-time PCR assay using gene-specific primers in SYBR green chemistry. The fold change in expression was calculated after normalization to β-tubulin for each condition (6).

Immunofluorescence staining of cells and tissue sections. TIME cells (uninfected and KSHV infected) were cultured on 8-chambered glass slides and fixed with 4% paraformaldehyde for 20 min at room temperature. The fixed cells were permeabilized using 0.2% Triton X-100 for 5 min, followed by blocking with Image-iT FX signaling enhancer (Life Technologies) for 20 min. Staining was done using specific primary and fluorescent Alexa Fluor-conjugated secondary antibodies as described previously (66, 68). BCBL-1 and BJAB cells were also cultured on multispot glass slides and stained similarly except the fixation and permeabilization steps, which were done by incubating the slides in ice-cold acetone for 10 min followed blocking and staining as described before (66).

Formalin-fixed, paraffin-embedded tissue section samples from healthy subjects and patients with Kaposi's sarcoma and primary effusion lymphoma were obtained from the AIDS and Cancer Specimen Resource (ACSR; San Francisco, CA). Tissue sections were deparaffinized with HistoChoice clearing reagent (Sigma) and rehydrated through ethanol to water. Antigen retrieval was performed by microwaving the tissue sections in 1 mmol/liter of EDTA (pH 8.0) for 15 min, followed by permeabilization, blocking, and staining with specific antibodies as described for TIME cells. The stained cells were visualized using a Nikon 80i fluorescence microscope. The relative fluorescence intensities were analyzed for three different fields with a minimum of 10 cells each with the MetaMorph pixel intensity calculator. Tissue sections were also stained using hematoxylin for observing tissue morphology.

Cell viability measurement. Viability and death of the cells were measured by using the MTT-based assay as per the manufacturer's instructions. Briefly, the cells were treated with MTT solution and incubated at 37°C until purple precipitate was clearly visible. The cells were then treated with detergent reagent and the absorbance was read at 570 nm in a Synergy HT microplate reader (BioTek Instruments).

Statistical analysis. All results are expressed as means ± standard deviations (SD) of at least three independent experiments to ensure reproducibility. Significant differences between samples were determined using two-tailed Student's *t* test. A *P* value of <0.05 was considered significant.

ACKNOWLEDGMENTS

This study was supported in part by Public Health Service grant CA 180758 and USF start-up funds to Bala Chandran.

We sincerely thank Robert Dickinson (Flow Cytometry Core Facility, RFUMS) for assisting with flow cytometry.

REFERENCES

1. Cesarman E, Chang Y, Moore PS, Said JW, Knowles DM. 1995. Kaposi's sarcoma-associated herpesvirus-like DNA sequences in AIDS-related body-cavity-based lymphomas. N Engl J Med 332:1186–1191. https://doi.org/10.1056/NEJM199505043321802.
2. Soulier J, Grollet L, Oksenhendler E, Cacoub P, Cazals-Hatem D, Babinet P, d'Agay MF, Clauvel JP, Raphael M, Degos L, Sigaux F. 1995. Kaposi's sarcoma-associated herpesvirus-like DNA sequences in multicentric Castleman's disease. Blood 86:1276–1280.
3. Damania B, Cesarman E. 2013. Kaposi's sarcoma-associated herpesvirus, vol 2, p 2080–2128. *In* Knipe DM, Howley PM, Cohen JI, Griffin DE, Lamb RA, Martin MA, Racaniello VR, Roizman B (ed), Fields virology, 6th ed. Lippincott Williams & Wilkins, Philadelphia, PA.
4. Schulz TF, Cesarman E. 2015. Kaposi sarcoma-associated herpesvirus: mechanisms of oncogenesis. Curr Opin Virol 14:116–128. https://doi.org/10.1016/j.coviro.2015.08.016.
5. Uppal T, Banerjee S, Sun Z, Verma SC, Robertson ES. 2014. KSHV LANA—the master regulator of KSHV latency. Viruses 6:4961–4998. https://doi.org/10.3390/v6124961.
6. Krishnan HH, Naranatt PP, Smith MS, Zeng L, Bloomer C, Chandran B. 2004. Concurrent expression of latent and a limited number of lytic genes with immune modulation and antiapoptotic function by Kaposi's sarcoma-associated herpesvirus early during infection of primary endothelial and fibroblast cells and subsequent decline of lytic gene expression. J Virol 78:3601–3620. https://doi.org/10.1128/JVI.78.7.3601-3620.2004.
7. Sharma-Walia N, Paul AG, Bottero V, Sadagopan S, Veettil MV, Kerur N, Chandran B. 2010. Kaposi's sarcoma associated herpes virus (KSHV) induced COX-2: a key factor in latency, inflammation, angiogenesis, cell survival and invasion. PLoS Pathog 6:e1000777. https://doi.org/10.1371/journal.ppat.1000777.
8. Naranatt PP, Krishnan HH, Svojanovsky SR, Bloomer C, Mathur S, Chandran B. 2004. Host gene induction and transcriptional reprogramming in Kaposi's sarcoma-associated herpesvirus (KSHV/HHV-8)-infected endothelial, fibroblast, and B cells: insights into modulation events early during infection. Cancer Res 64:72–84. https://doi.org/10.1158/0008-5472.CAN-03-2767.
9. Gasperini P, Sakakibara S, Tosato G. 2008. Contribution of viral and cellular cytokines to Kaposi's sarcoma-associated herpesvirus pathogenesis. J Leukoc Biol 84:994–1000. https://doi.org/10.1189/jlb.1107777.
10. Li X, Feng J, Sun R. 2011. Oxidative stress induces reactivation of Kaposi's sarcoma-associated herpesvirus and death of primary effusion lymphoma cells. J Virol 85:715–724. https://doi.org/10.1128/JVI.01742-10.
11. Ye F, Zhou F, Bedolla RG, Jones T, Lei X, Kang T, Guadalupe M, Gao S-J. 2011. Reactive oxygen species hydrogen peroxide mediates Kaposi's sarcoma-associated herpesvirus reactivation from latency. PLoS Pathog 7:e1002054. https://doi.org/10.1371/journal.ppat.1002054.
12. Guilluy C, Zhang Z, Bhende PM, Sharek L, Wang L, Burridge K, Damania B. 2011. Latent KSHV infection increases the vascular permeability of human endothelial cells. Blood 118:5344–5354. https://doi.org/10.1182/blood-2011-03-341552.
13. Ma Q, Cavallin LE, Leung HJ, Chiozzini C, Goldschmidt-Clermont PJ, Mesri EA. 2013. A role for virally induced reactive oxygen species in Kaposi's sarcoma herpesvirus tumorigenesis. Antioxid Redox Signal 18:80–90. https://doi.org/10.1089/ars.2012.4584.
14. Bottero V, Chakraborty S, Chandran B. 2013. Reactive oxygen species are induced by Kaposi's sarcoma-associated herpesvirus early during primary infection of endothelial cells to promote virus entry. J Virol 87:1733–1749. https://doi.org/10.1128/JVI.02958-12.
15. Kumar B, Chandran B. 2016. KSHV entry and trafficking in target cells—hijacking of cell signal pathways, actin and membrane dynamics. Viruses 8:E305.
16. Naranatt PP, Akula SM, Zien CA, Krishnan HH, Chandran B. 2003. Kaposi's sarcoma-associated herpesvirus induces the phosphatidylinositol 3-kinase-PKC-zeta-MEK-ERK signaling pathway in target cells early during infection: implications for infectivity. J Virol 77:1524–1539. https://doi.org/10.1128/JVI.77.2.1524-1539.2003.
17. Sharma-Walia N, Raghu H, Sadagopan S, Sivakumar R, Veettil MV, Naranatt PP, Smith MM, Chandran B. 2006. Cyclooxygenase 2 induced by Kaposi's sarcoma-associated herpesvirus early during in vitro infection of target cells plays a role in the maintenance of latent viral gene expression. J Virol 80:6534–6552. https://doi.org/10.1128/JVI.00231-06.
18. Sadagopan S, Sharma-Walia N, Veettil MV, Raghu H, Sivakumar R, Bottero V, Chandran B. 2007. Kaposi's sarcoma-associated herpesvirus induces sustained NF-kappaB activation during de novo infection of primary human dermal microvascular endothelial cells that is essential for viral gene expression. J Virol 81:3949–3968. https://doi.org/10.1128/JVI.02333-06.
19. Sharma-Walia N, Patel K, Chandran K, Marginean A, Bottero V, Kerur N, Paul AG. 2012. COX-2/PGE2: molecular ambassadors of Kaposi's sarcoma-associated herpes virus oncoprotein-v-FLIP. Oncogenesis 1:e5. https://doi.org/10.1038/oncsis.2012.5.
20. Moi P, Chan K, Asunis I, Cao A, Kan YW. 1994. Isolation of NF-E2-related factor 2 (Nrf2), a NF-E2-like basic leucine zipper transcriptional activator that binds to the tandem NF-E2/AP1 repeat of the beta-globin locus control region. Proc Natl Acad Sci U S A 91:9926–9930. https://doi.org/10.1073/pnas.91.21.9926.
21. Baird L, Dinkova-Kostova AT. 2011. The cytoprotective role of the Keap1-Nrf2 pathway. Arch Toxicol 85:241–272. https://doi.org/10.1007/s00204-011-0674-5.
22. Motohashi H, Yamamoto M. 2004. Nrf2-Keap1 defines a physiologically important stress response mechanism. Trends Mol Med 10:549–557. https://doi.org/10.1016/j.molmed.2004.09.003.
23. Chen W, Sun Z, Wang XJ, Jiang T, Huang Z, Fang D, Zhang DD. 2009. Direct interaction between Nrf2 and p21(Cip1/WAF1) upregulates the Nrf2-mediated antioxidant response. Mol Cell 34:663–673. https://doi.org/10.1016/j.molcel.2009.04.029.
24. Komatsu M, Kurokawa H, Waguri S, Taguchi K, Kobayashi A, Ichimura Y, Sou YS, Ueno I, Sakamoto A, Tong KI, Kim M, Nishito Y, Iemura S, Natsume T, Ueno T, Kominami E, Motohashi H, Tanaka K, Yamamoto M. 2010. The selective autophagy substrate p62 activates the stress responsive transcription factor Nrf2 through inactivation of Keap1. Nat Cell Biol 12:213–223. https://doi.org/10.1038/ncb2021.
25. Purdom-Dickinson SE, Sheveleva EV, Sun H, Chen QM. 2007. Translational control of nrf2 protein in activation of antioxidant response by oxidants. Mol Pharmacol 72:1074–1081. https://doi.org/10.1124/mol.107.035360.
26. Gjyshi O, Bottero V, Veettil MV, Dutta S, Singh VV, Chikoti L, Chandran B. 2014. Kaposi's sarcoma-associated herpesvirus induces Nrf2 during de novo infection of endothelial cells to create a microenvironment con-

ducive to infection. PLoS Pathog 10:e1004460. https://doi.org/10.1371/journal.ppat.1004460.
27. Gjyshi O, Flaherty S, Veettil MV, Johnson KE, Chandran B, Bottero V. 2015. Kaposi's sarcoma-associated herpesvirus induces Nrf2 activation in latently infected endothelial cells through SQSTM1 phosphorylation and interaction with polyubiquitinated Keap1. J Virol 89:2268–2286. https://doi.org/10.1128/JVI.02742-14.
28. Gjyshi O, Roy A, Dutta S, Veettil MV, Dutta D, Chandran B. 2015. Activated Nrf2 interacts with Kaposi's sarcoma-associated herpesvirus latency protein LANA-1 and host protein KAP1 to mediate global lytic gene repression. J Virol 89:7874–7892. https://doi.org/10.1128/JVI.00895-15.
29. Anglesio MS, Evdokimova V, Melnyk N, Zhang L, Fernandez CV, Grundy PE, Leach S, Marra MA, Brooks-Wilson AR, Penninger J, Sorensen PH. 2004. Differential expression of a novel ankyrin containing E3 ubiquitin-protein ligase, Hace1, in sporadic Wilms' tumor versus normal kidney. Hum Mol Genet 13:2061–2074. https://doi.org/10.1093/hmg/ddh215.
30. Zhang L, Anglesio MS, O'Sullivan M, Zhang F, Yang G, Sarao R, Mai PN, Cronin S, Hara H, Melnyk N, Li L, Wada T, Liu PP, Farrar J, Arceci RJ, Sorensen PH, Penninger JM. 2007. The E3 ligase HACE1 is a critical chromosome 6q21 tumor suppressor involved in multiple cancers. Nat Med 13:1060–1069. https://doi.org/10.1038/nm1621.
31. Tang D, Xiang Y, De Renzis S, Rink J, Zheng G, Zerial M, Wang Y. 2011. The ubiquitin ligase HACE1 regulates Golgi membrane dynamics during the cell cycle. Nat Commun 2:501. https://doi.org/10.1038/ncomms1509.
32. Daugaard M, Nitsch R, Razaghi B, McDonald L, Jarrar A, Torrino S, Castillo-Lluva S, Rotblat B, Li L, Malliri A, Lemichez E, Mettouchi A, Berman JN, Penninger JM, Sorensen PH. 2013. Hace1 controls ROS generation of vertebrate Rac1-dependent NADPH oxidase complexes. Nat Commun 4:2180. https://doi.org/10.1038/ncomms3180.
33. Rotblat B, Southwell AL, Ehrnhoefer DE, Skotte NH, Metzler M, Franciosi S, Leprivier G, Somasekharan SP, Barokas A, Deng Y, Tang T, Mathers J, Cetinbas N, Daugaard M, Kwok B, Li L, Carnie CJ, Fink D, Nitsch R, Galpin JD, Ahern CA, Melino G, Penninger JM, Hayden MR, Sorensen PH. 2014. HACE1 reduces oxidative stress and mutant Huntingtin toxicity by promoting the NRF2 response. Proc Natl Acad Sci U S A 111:3032–3037. https://doi.org/10.1073/pnas.1314421111.
34. Ehrnhoefer DE, Southwell AL, Sivasubramanian M, Qiu X, Villanueva EB, Xie Y, Waltl S, Anderson L, Fazeli A, Casal L, Felczak B, Tsang M, Hayden MR. 2018. HACE1 is essential for astrocyte mitochondrial function and influences Huntington disease phenotypes in vivo. Hum Mol Genet 27:239–253. https://doi.org/10.1093/hmg/ddx394.
35. Mallery SR, Pei P, Landwehr DJ, Clark CM, Bradburn JE, Ness GM, Robertson FM. 2004. Implications for oxidative and nitrative stress in the pathogenesis of AIDS-related Kaposi's sarcoma. Carcinogenesis 25:597–603. https://doi.org/10.1093/carcin/bgh042.
36. Tortola L, Nitsch R, Bertrand MJM, Kogler M, Redouane Y, Kozieradzki I, Uribesalgo I, Fennell LM, Daugaard M, Klug H, Wirnsberger G, Wimmer R, Perlot T, Sarao R, Rao S, Hanada T, Takahashi N, Kernbauer E, Demiroz D, Lang M, Superti-Furga G, Decker T, Pichler A, Ikeda F, Kroemer G, Vandenabeele P, Sorensen PH, Penninger JM. 2016. The tumor suppressor Hace1 is a critical regulator of TNFR1-mediated cell fate. Cell Rep 16:3414. https://doi.org/10.1016/j.celrep.2016.08.072.
37. Zhang DD. 2006. Mechanistic studies of the Nrf2-Keap1 signaling pathway. Drug Metab Rev 38:769–789. https://doi.org/10.1080/03602530600971974.
38. Prestera T, Talalay P, Alam J, Ahn YI, Lee PJ, Choi AM. 1995. Parallel induction of heme oxygenase-1 and chemoprotective phase 2 enzymes by electrophiles and antioxidants: regulation by upstream antioxidant-responsive elements (ARE). Mol Med 1:827–837. https://doi.org/10.1007/BF03401897.
39. Ren D, Villeneuve NF, Jiang T, Wu T, Lau A, Toppin HA, Zhang DD. 2011. Brusatol enhances the efficacy of chemotherapy by inhibiting the Nrf2-mediated defense mechanism. Proc Natl Acad Sci U S A 108:1433–1438. https://doi.org/10.1073/pnas.1014275108.
40. Newsholme P, Lima MMR, Procopio J, Pithon-Curi TC, Doi SQ, Bazotte RB, Curi R. 2003. Glutamine and glutamate as vital metabolites. Braz J Med Biol Res 36:153–163. https://doi.org/10.1590/S0100-879X2003000200002.
41. Valiya Veettil M, Dutta D, Bottero V, Bandyopadhyay C, Gjyshi O, Sharma-Walia N, Dutta S, Chandran B. 2014. Glutamate secretion and metabotropic glutamate receptor 1 expression during Kaposi's sarcoma-associated herpesvirus infection promotes cell proliferation. PLoS Pathog 10:e1004389. https://doi.org/10.1371/journal.ppat.1004389.
42. Sanchez EL, Carroll PA, Thalhofer AB, Lagunoff M. 2015. Latent KSHV infected endothelial cells are glutamine addicted and require glutaminolysis for survival. PLoS Pathog 11:e1005052. https://doi.org/10.1371/journal.ppat.1005052.
43. Cetinbas N, Daugaard M, Mullen AR, Hajee S, Rotblat B, Lopez A, Li A, DeBerardinis RJ, Sorensen PH. 2015. Loss of the tumor suppressor Hace1 leads to ROS-dependent glutamine addiction. Oncogene 34:4005–4010. https://doi.org/10.1038/onc.2014.316.
44. Singh VV, Kerur N, Bottero V, Dutta S, Chakraborty S, Ansari MA, Paudel N, Chikoti L, Chandran B. 2013. Kaposi's sarcoma-associated herpesvirus latency in endothelial and B cells activates gamma interferon-inducible protein 16-mediated inflammasomes. J Virology 87:4417–4431. https://doi.org/10.1128/JVI.03282-12.
45. Muralidhar S, Pumfery AM, Hassani M, Sadaie MR, Azumi N, Kishishita M, Brady JN, Doniger J, Medveczky P, Rosenthal LJ. 1998. Identification of kaposin (open reading frame K12) as a human herpesvirus 8 (Kaposi's sarcoma-associated herpesvirus) transforming gene. J Virol 72:4980–4988.
46. Chen X, Cheng L, Jia X, Zeng Y, Yao S, Lv Z, Qin D, Fang X, Lei Y, Lu C. 2009. Human immunodeficiency virus type 1 Tat accelerates Kaposi sarcoma-associated herpesvirus kaposin A-mediated tumorigenesis of transformed fibroblasts in vitro as well as in nude and immunocompetent mice. Neoplasia 11:1272–1284. https://doi.org/10.1593/neo.09494.
47. Kliche S, Nagel W, Kremmer E, Atzler C, Ege A, Knorr T, Koszinowski U, Kolanus W, Haas J. 2001. Signaling by human herpesvirus 8 kaposin A through direct membrane recruitment of cytohesin-1. Mol Cell 7:833–843. https://doi.org/10.1016/S1097-2765(01)00227-1.
48. Shah AM, Channon KM. 2004. Free radicals and redox signalling in cardiovascular disease. Heart 90:486–487. https://doi.org/10.1136/hrt.2003.029389.
49. Devasagayam TP, Tilak JC, Boloor KK, Sane KS, Ghaskadbi SS, Lele RD. 2004. Free radicals and antioxidants in human health: current status and future prospects. J Assoc Physicians India 52:794–804.
50. Finkel T. 1998. Oxygen radicals and signaling. Curr Opin Cell Biol 10:248–253. https://doi.org/10.1016/S0955-0674(98)80147-6.
51. Cooke MS, Evans MD, Dizdaroglu M, Lunec J. 2003. Oxidative DNA damage: mechanisms, mutation, and disease. FASEB J 17:1195–1214. https://doi.org/10.1096/fj.02-0752rev.
52. Schwarz KB. 1996. Oxidative stress during viral infection: a review. Free Radic Biol Med 21:641–649. https://doi.org/10.1016/0891-5849(96)00131-1.
53. Ye F, Gao S-J. 2011. A novel role of hydrogen peroxide in Kaposi sarcoma-associated herpesvirus reactivation. Cell Cycle 10:3237–3238. https://doi.org/10.4161/cc.10.19.17299.
54. Wang JF, Zhang X, Chandran B, Groopman JE. 2004. Human herpesvirus-8 (HHV-8/KSHV) induces reactive oxygen species in endothelial cells that facilitate virus infection. Blood 104:605.
55. Huttemann M, Lee I, Grossman LI, Doan JW, Sanderson TH. 2012. Phosphorylation of mammalian cytochrome c and cytochrome c oxidase in the regulation of cell destiny: respiration, apoptosis, and human disease. Adv Exp Med Biol 748:237–264. https://doi.org/10.1007/978-1-4614-3573-0_10.
56. Bedard K, Krause KH. 2007. The NOX family of ROS-generating NADPH oxidases: physiology and pathophysiology. Physiol Rev 87:245–313. https://doi.org/10.1152/physrev.00044.2005.
57. Ramezani A, Nahad MP, Faghihloo E. 2018. The role of Nrf2 transcription factor in viral infection. J Cell Biochem 119:6366–6382. https://doi.org/10.1002/jcb.26897.
58. Yageta Y, Ishii Y, Morishima Y, Masuko H, Ano S, Yamadori T, Itoh K, Takeuchi K, Yamamoto M, Hizawa N. 2011. Role of Nrf2 in host defense against influenza virus in cigarette smoke-exposed mice. J Virol 85:4679–4690. https://doi.org/10.1128/JVI.02456-10.
59. Lee J, Koh K, Kim YE, Ahn JH, Kim S. 2013. Upregulation of Nrf2 expression by human cytomegalovirus infection protects host cells from oxidative stress. J Gen Virol 94:1658–1668. https://doi.org/10.1099/vir.0.052142-0.
60. Satoh H, Moriguchi T, Takai J, Ebina M, Yamamoto M. 2013. Nrf2 prevents initiation but accelerates progression through the Kras signaling pathway during lung carcinogenesis. Cancer Res 73:4158–4168. https://doi.org/10.1158/0008-5472.CAN-12-4499.
61. Sykiotis GP, Bohmann D. 2010. Stress-activated cap'n'collar transcription factors in aging and human disease. Sci Signal 3:re3. https://doi.org/10.1126/scisignal.3112re3.
62. Kumar B, Roy A, Veettil MV, Chandran B. 2018. Insight into the roles of

E3 ubiquitin ligase c-Cbl, ESCRT machinery, and host cell signaling in Kaposi's sarcoma-associated herpesvirus entry and trafficking. J Virol 92:e01376-17. https://doi.org/10.1128/JVI.01376-17.
63. Venugopal R, Jaiswal AK. 1996. Nrf1 and Nrf2 positively and c-Fos and Fra1 negatively regulate the human antioxidant response element-mediated expression of NAD(P)H:quinone oxidoreductase1 gene. Proc Natl Acad Sci U S A 93:14960–14965. https://doi.org/10.1073/pnas.93.25.14960.
64. Sanchez EL, Pulliam TH, Dimaio TA, Thalhofer AB, Delgado T, Lagunoff M. 2017. Glycolysis, glutaminolysis, and fatty acid synthesis are required for distinct stages of Kaposi's sarcoma-associated herpesvirus lytic replication. J Virol 91:e02237-16. https://doi.org/10.1128/JVI.02237-16.
65. Zhu Y, Li T, Ramos da Silva S, Lee J-J, Lu C, Eoh H, Jung JU, Gao S-J. 2017. A critical role of glutamine and asparagine γ-nitrogen in nucleotide biosynthesis in cancer cells hijacked by an oncogenic virus. mBio 8:e01179-17. https://doi.org/10.1128/mBio.01179-17.
66. Kumar B, Dutta D, Iqbal J, Ansari MA, Roy A, Chikoti L, Pisano G, Veettil MV, Chandran B. 2016. ESCRT-I protein Tsg101 plays a role in the post-macropinocytic trafficking and infection of endothelial cells by Kaposi's sarcoma-associated herpesvirus. PLoS Pathog 12:e1005960. https://doi.org/10.1371/journal.ppat.1005960.
67. Tiscornia G, Singer O, Verma IM. 2006. Production and purification of lentiviral vectors. Nat Protoc 1:241. https://doi.org/10.1038/nprot.2006.37.
68. Veettil MV, Kumar B, Ansari MA, Dutta D, Iqbal J, Gjyshi O, Bottero V, Chandran B. 2016. ESCRT-0 component Hrs promotes macropinocytosis of Kaposi's sarcoma-associated herpesvirus in human dermal microvascular endothelial cells. J Virol 90:3860–3872. https://doi.org/10.1128/JVI.02704-15.